University of South Carolina

Scholar Commons

2017

Fast Scan Cyclic Voltammetry for Real-Time Metal Speciation Analysis

Hettige. M. Thushani Siriwardhane
University of South Carolina

FAST SCAN CYCLIC VOLTAMMETRY FOR REAL-TIME METAL SPECIATION ANALYSIS

by

Hettige. M. Thushani Siriwardhane

Bachelor of Science

University of Colombo, 2011

_____

Submitted in Partial Fulfillment of the Requirements

For the Degree of Doctor of Philosophy in

Chemistry

College of Arts and Sciences

University of South Carolina

2017

Accepted by:

Parastoo Hashemi, Major Professor

Susan D. Richardson, Chairman, Examining Committee

John J. Lavigne, Committee Member

Beth Krizek, Committee Member

Cheryl L. Addy, Vice Provost and Dean of the Graduate School

DEDICATION

This work is dedicated to my loving parents, my sister, my husband, and the little miracle of my life, whose steadfast care and guidance made it possible to complete this work.

ACKNOWLEDGEMENTS

First and foremost, I would like to express my sincere gratitude and appreciation to my advisor and mentor, Dr. Parastoo Hashemi. I consider joining her lab one of the best decisions I made during my grad school career. Her guidance and motivation have been crucial to realizing my potentials and to becoming an independent and confident scientist. Through the ups and downs of grad school, she was always supportive and guided me on the right track. Her enthusiasm and courage towards science and personal life always motivated me to achieve my goals. Thank you Parry for your understanding, patience, and guidance in helping me to become the person who I am today.

I am very grateful to the members of my dissertation committee, Dr. Richardson, Dr. Lavigne and Dr. Krizek for their advices, insights and especially for their understanding. I would also like to thank my former committee members at Wayne state university, Dr. Poole and Dr. Cha for their invaluable comments and intellectual ideas. I would especially like to thank Dr. McElmurry at Wayne State University for his unwavering support and inspiration throughout the years. I also want to thank all the Hashemi lab members, both past and present for the support and friendship you all have shown me. My special thanks go to Pavithra, Sheirly, Rachel, Kevin, Jordan, Aya, Srimal, Shane, Alyssa, Rhiannon,

iv

Thank you both for giving me a reason to continue to rise higher, so that we can overcome every challenge together.

ABSTRACT

Electrochemistry is a powerful analytical tool that has been widely used to detect trace metals in natural systems. However, studying the speciation of metals during dynamic events, such as storms and floods, is analytically challenging due to the limited temporal resolution of traditional electrochemical techniques. Additionally, most techniques report the total metal concentration (both complexed and free) that does not reflect the toxicity of these metals, which arise mostly from the free state. To overcome these issues, we previously pioneered the use of fast scan cyclic voltammetry (FSCV) to measure free copper (Cu(II)) and lead (Pb(II)) in real-time in laboratory test solutions. In the current work, we describe the application of our technique measuring different metals in various systems. First, we perform a proof-of-principle complexation study between Cu(II) and a model set of ligands to showcase the feasibility of FSCV to provide complexation information in real-time. We then extend this study towards developing an on-site speciation sensor by developing a mathematical relationship between FSCV response, free Cu(II) concentration, and the complexation constant (K_f) of a range of model ligands. Finally, we apply our technique to rapidly characterize metals with high standard reduction potentials such as Ca(II), Al(III), Zn(II), and Mg(II), that are difficult to analyze via traditional electrochemical techniques. Together, our data showcase the power

of FSCV to rapidly provide speciation information for a variety of metals that can be used in the development of cheap, eco-friendly, handheld, and portable on-site metal speciation sensors in the near future.

PREFACE

This dissertation is based closely on the following refereed publications:

Chapter 2: Siriwardhane, T.; Sulkanen, A.; Tremonti, A.; McElmurry, S. P.; Hashemi, P.: "Real-time Voltammetric Characterization of Cu(II) Complexation"., Analytical Chemistry 2016 88 (15), 7603-7608

Chapter 3: Pathirathna, P.; Siriwardhane, T.; Morgan S.L.; McElmurry, S. P.; Hashemi, P.; "Fast voltammetry of metals at carbon-fiber microelectrodes: ultra rapid determination of solution formation constants"., Analyst 2016, 141, 6432

Chapter 4: Pathirathna, P.; Siriwardhane, T.; Morgan S.L.; McElmurry, S. P.; Hashemi, P.: "Fast voltammetry of metals at carbon-fiber microelectrodes: towards a real time speciation sensor". Analyst 2016, 141, 6432

Chapter 5: Siriwardhane, T.; Pathirathna, P.; Hashemi, P.: "Rapid Electrochemical Analysis of Ca(II), Al(III), Zn(II), Mg(II) via Fast-Scan Cyclic Voltammetry at Carbon-Fiber Microelectrodes" – In preparation - Analytical Chemistry

TABLE OF CONTENTS

LIST OF TABLES

LIST OF FIGURES

CHAPTER 1

INTRODUCTION

1.1 Metal Toxicity

Metal homeostasis in natural systems is constantly changing due to industrial, domestic, agricultural, medical and technological activities.[1] Additionally, metals are considered a major pollutant, raising ecological and public health concerns over the past few decades. Metals are found naturally; metal pollution events occur due to anthropogenic activities such as mining, smelting, agricultural products, and natural events like weathering, volcanic eruptions, storms and flooding.[2] In order to study metals in natural systems, analytical techniques, capable of real time metal detection mainly in biological and environmental matrices, are vital. In this chapter, metal pollution in biological and environmental systems is discussed. Additionally, existing analytical systems for metal analysis in these systems are described.

1.1.1 Metal Toxicity in Biological Systems

Even though metals show adverse health effects when present at high concentrations, some of these metals have biological importance to humans and plants within a given threshold. Metals such as cobalt (Co), copper (Cu), chromium (Cr), iron (Fe), magnesium (Mg), manganese (Mn), nickel (Ni), zinc

(Zn) are essential for different physiological functions.[1,2] Most of these metals play a vital role in different enzyme pathways, and a deficiency or high levels could lead to dysfunctions.[3,4] For example, Cu serves as a co-factor for multiple enzymes. Hence, its deficiency could alter a number of enzymatic pathways, while high exposure is linked to cell damage causing Wilson's disease in humans.[5,6] Most diseases related to metals are traditionally characterized by physiological symptoms, however a biomarker would infinitely aid diagnosis and treatment.

1.1.2 Metal Toxicity in Environmental Systems

The removal of excess metals from environmental systems is a complex effort. Natural lakes, rivers, coastal waters, other aquatic reservoirs and soil are often polluted.[7] Metals such as lead (Pb), arsenic (As), cadmium (Cd), copper (Cu), aluminium (Al), mercury (Hg) are harmful to humans.[1] These metals show complicated behavior in aqueous systems since their speciation can change dynamically. Most metal detection techniques have time scales ranging from a few seconds to minutes and most report the total metal concentration when it is the free concentration that is important for mitigation purposes.[8,9] Risk assessment and metal mitigation in rapidly fluctuating systems should be evaluated in real-time, however, there are no methods available which can provide real-time information.

1.2 Techniques for Heavy Metal Ion Detection

A variety of techniques are available for detection of metals in various natural systems. The two most commonly used are spectroscopic and

electrochemical techniques. The choice of which technique to use for specific applications is based on sensitivity, selectivity, limits of detection, costs and ease of use. Different spectroscopic and electrochemical techniques are described in the following subsections.

1.2.1 Spectroscopic Methods

Spectroscopic methods are the most widely used for analysis of metals in environmental systems. Traditional quantitative spectroscopic methods include atomic absorption spectroscopy, inductively coupled plasma mass spectrometry (ICP-MS), cold vapor atomic fluorescence spectrometry, X-ray fluorescence and neutron activation analysis.[10-12] These methods are versatile for a large number of metals and posses high sensitivity and low limit of detection (LOD). However, these methods suffer from expensive and sophisticated instrumentation requirements, low portability, and high turnover time. Ultimately, the main disadvantage of these methods for metal analysis in environmental solutions is the multi-step sample preparation, which can change the speciation of metals in the solution. As discussed above, the total metal concentration does not adequately represent the pollution level. These drawbacks make spectroscopy challenging for *in situ* analysis of metals. Hence, a real-time technique, that can detect free metal ions in natural solutions, is required to provide meaningful data to improve metal remediation methods for contaminated sites. An electrochemical approach provides an alternative to address these challenges, as discussed in the next section.

1.2.2 Electrochemical Methods

Recently, there has been a great deal of effort in the development of electrochemical techniques capable of metal ion detection in different natural systems. The inherent portability, low cost, and miniaturized equipment make electrochemical techniques dominant in the field of *in situ* metal analysis. Moreover, electrochemical systems provide faster measurements that can deliver significant speciation information which can be used for toxicity evaluations. The key electrochemical techniques that have been employed in the field are: stripping voltammetry (both anodic and cathodic), and electrochemical sensors (such as ion selective electrodes).

Anodic stripping voltammetry (ASV), is widely used in the metal analysis field due to its high sensitivity in trace metal analysis,[13,14] The basic experimental outline can be seen in figure 1.1. ASV consists of three steps, each of which can be optimized based on the analyte of interest. The first step is a cleaning step in which the electrode is held at a more positive potential than the oxidation potential of the analyte, to remove or discharge all the impurities from the electrode surface. The second step is the electrodeposition and equllibration step wherein the potential switches to a more negative potential than the reduction potential of the species and is held constant for a period of time in order to preconcentrating the analyte of interest. This occurs in a stirred solution to increase the mass transport to the electrode. The final step is an oxidation step where the potential ramps to the positive direction to strip off the deposited metal/analyte from the surface. An unstirred solution is employed in this step.

A variety of electrode materials can be used in the ASV, however, mercury electrodes are most commonly employed due to their ability to form a stable amalgam with metals.[15,16] Longer deposition times are utilized in ASV to increase the preconcentration of the metal on the surface, resulting in higher sensitivity. Although the above factors provide high sensitivity for metals in ASV, they also limit its use for *in situ* monitoring of metals. Mercury is an environmental toxin and therefore unsuitable for use in natural systems. Additionally, the preconcentration time (minutes) required for high sensitivity in ASV decreases the temporal resolution of the technique, limiting its use in real time analysis.
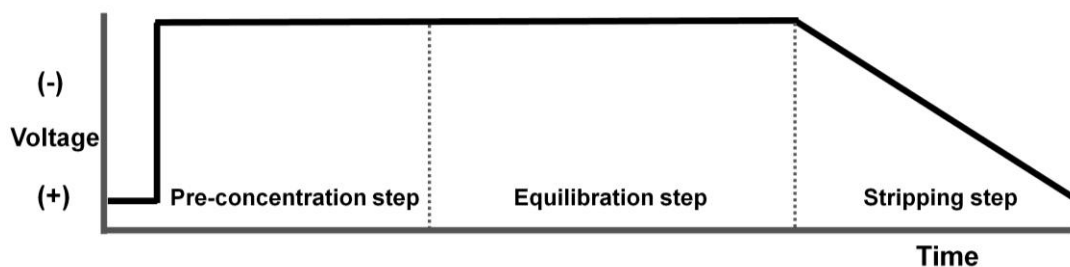
Figure 1.1. Schematic representation of anodic stripping voltammetry (ASV)

In 2000, Wang *et al.* introduced bismuth electrodes as an alternative to mercury for the *in situ* analysis of trace metals.[17] Bismuth is capable of forming a fused alloy similar to a mercury amalgam which facilitates the nucleation process for better analysis of trace metals.[18,19] However, the narrow potential window associate with bismuth electrodes limits its use to metals which have high reduction potentials than bismuth. Bismuth electrodes also require a preconcentration step, making it less favorable for real-time analysis.[18]

Another widely used electrochemical technique in environmental analysis is ion selective electrodes (ISE). These electrodes are comprised of an indicator electrode with a membrane selective for the analyte of interest and a reference electrode. The potential change across the selective membrane is measured as a function of potential based on the concentration of the analyte. Depending on the nature of the binding site, ISE can be categorized into various classes: glass membrane, solid-state membrane, liquid membrane, or modified/compound membrane electrodes.[20] The main advantages of ISEs are that they produce non-destructive measurements which are unaffected by the color or the turbidity of the solution. They also have good selectivity, sensitivity and portability which makes them useful for field analysis.[21] However, the poor stability and low temporal resolution of ISEs make them unsuitable for the analysis of dynamic events in natural systems.[22] To overcome the challenges traditionally associated with metal analysis, Hashemi *et. al.* introduced fast scan cyclic voltammetry to analyze trace metals in solutions in 2012.

1.2.2.1 Fast Scan Cyclic Voltammetry at Carbon Fiber Microelectrodes

An ideal on-site real-time metal analysis technique requires a number of characteristics, including sensitivity, selectivity, stability, and speed. Fast scan cyclic voltammetry (FSCV) possess these characteristics and is capable of metal analysis.

In 1980, Julian Milar and colleagues first introduced FSCV in neuroscience applications[23] and for over three decades, it has been one of the

6

most widely accepted electroanalytical techniques among neuroscientists to analyze real-time neurotransmitter behavior, biological amines and other electroactive molecules in the brain. FSCV is an extension of classical cyclic voltammetry with high scan rates (100 V s^{-1} to 2500 V s^{-1}). Higher scan rates, together with a waveform application frequency of 10 Hz, produce measurements in milliseconds, allowing for real-time analysis. Since high scan rates produce large non Faradaic currents across the electrode surface, the technique is modified to integrate background subtraction to eliminate this interfering signal.[24]

FSCV employs a specific waveform at a specific frequency for a given analyte. The electrode is held at the resting potential between cycles, allowing analytes to adsorb onto the electrode. During the cathodic and anodic waves, the adsorbed analyte will repeatedly be reduced and oxidized on the electrode creating an electron flow in the solution. The resulting Faradaic current is measured after background subtraction. During this process, an analyte specific cyclic voltammogram (CV) is generated that can be used for qualitative analysis. For data visualization purposes, a 3D plot, known as a color plot, is digitally constructed through stacking a series of CVs in the sequence of time. The color plot provides qualitative and quantitative information of the specific analyte in the solution.

Carbon fiber microelectrodes (CFMs) are used in FSCV analysis. CFMs can be fabricated in different ways, either by insulating a single carbon fiber in a glass capillary sealed in one edge and trimmed to a required length (25-150 µM) **(Figure 1.2)** to form a cylindrical electrode or by sealing the edge with epoxy and

polishing it to create a disc electrode. The features of CFMs include excellent kinetic properties which causes minimal background noise compared to other electrode materials, an oxygen rich surface that promotes rapid adsorption of charged molecules to its surface, and biocompatibility, among others.[26] Additionally, as these carbon fibers are on the micron scale, hemispherical diffusion inherently promotes an increased mass transfer of the analyte to the electrode surface. The micron dimensions also allow more accuracy, especially for *in vivo* measurements, due to less disturbance and damage to cells.[27,28] In 2012, our lab pioneered the application of FSCV at CFMs to monitor the trace metals Cu(II) and Pb(II).[29,30]
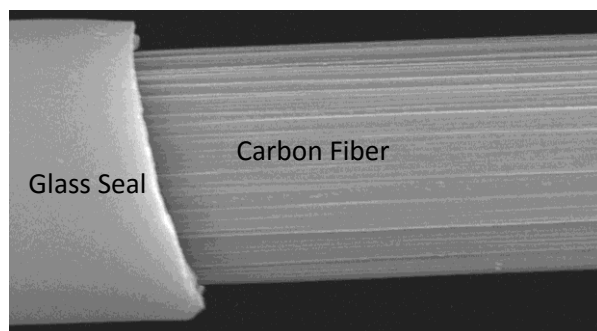
Figure 1.2. SEM image of a carbon-fiber microelectrode

1.2.2.2 Fast Scan Controlled Adsorption Voltammetry

Although FSCV is a powerful analytical tool to quantify molecules *in vitro* and *in vivo*, this method is restricted from directly measuring the ambient levels of molecules due to the requirement of background subtraction to remove the large non-Faradaic current. Therefore, FSCV is only capable of detecting rapid changes that happen in a given system. In 2014, a collaboration between the

Hashemi and Heien labs, has addressed this limitation by introducing an extended version of FSCV, known as fast scan controlled adsorption voltammetry (FSCAV).[31]
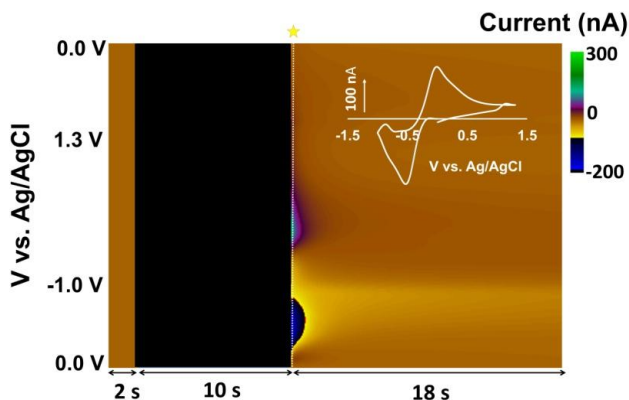
Figure 1.3. A representative color plot of a FSCAV analysis of Cu(II). First 2 s represents the minimal adsorption while the adsorption happens during the next 10 s (black box). The inset shows the first CV that arises after switching back the waveform.

FSCAV follows three basic steps. During the first step, an analyte specific waveform is applied at a high waveform application frequency (typically 100 Hz) to minimize adsorption for 2 seconds. In the next step, a constant potential, typically the resting potential of the specific waveform, is applied to the electrode for a controlled period. During this step, the analyte adsorbs onto the electrode surface until it reaches equilibrium. In the final step, the analyte specific waveform is re-applied, and adsorbed molecules undergo the same redox process as in FSCV. The first file of the collected CVs during the final step contain raw information of the total adsorbed analyte. Upon integration,the reduction/oxidation peak of the fist CV collected is converted to surface concentration via Faraday's law. Further, adsorption isotherm profiles can be

9

generated and equilibrium constants for adsorption onto CFM for each analyte can be calculated using an adsorption isotherm.

1.3 Scope of the dissertation

Metal analysis in our ecosystem is considered an important topic for analytical chemists. Although spectroscopic and electrochemical techniques have been employed, few techniques are capable of providing real-time speciation information. In 2012, our group initiated the real-time characterization of Cu(II) via FSCV at CFMs. In this dissertation, I investigate other metals, mainly ecologically problematic and difficult to detect metals such as Al(III), Ca(II), Zn(II), and Mg(II). I explored the real-time complexation of these metals to gain important speciation information. The outline of my dissertation is described below.

Chapter 1: Introduction

Chapter 2: This chapter concentrates on the application of FSCV to study the real-time binding of Cu(II) with a model set of ligands in a MOPS medium. A hydrodynamic model was developed to assess the mixing of Cu(II) in a constantly stirred solution. Finally, a thermodynamic model was employed to accurately monitor real-time complexation processes with good sensitivity via five model ligands.

Chapter 3: The effects of Cu(II) complexation with a variety of ligands on the FSCV response are interrogated. We chose 15 ligands that have differing binding abilities, mimicking the full range of complexation equilibria observed in

natural waters. We demonstrated that the surrounding matrix does not affect the adsorption properties of Cu(II) onto CFM by studying the adsorption profiles of Cu(II) in the presence of these ligands via FSCAV. We developed a nonlinear least square approach to accurately describe the relationship between Cu(II) FSCV signal and Cu(II)-ligand formation constants. This correlation provided proof of principle that our technique is capable of providing speciation information accurately.

Chapter 4: An expanded study detailed in chapter 3 is described that can report free Cu(II) and developed a model that relates free Cu(II) and the formation constant of Cu(II)-ligands. We assessed a ground water solution spiked with Cu(II) via the developed model and validated using commercially available Cu(II) ISE.

Chapter 5: This chapter presents a direct electrochemical approach to detect metals with high standard reduction potentials such as Ca(II), Al(III), Zn(II), Mg(II) via FSCV at CFMs. We constructed adsorption profiles for each metal via FSCAV and validated them by comparing their order of adsorption sequence to literature reported sequence for these metals on activated carbon. A proof of principle study using two model ligands BAPTA and EDTA showed that these metals can be quantified via FSCV and provide meaningful speciation information in real-time without any time consuming additional indirect processes. Chapter 6: The final chapter summarizes the conclusions of the research work and highlights future directions.

1.4 References

(1) Tchounwou, P. B.; Yedjou, C. G.; Patlolla, A. K.; Sutton, D. J. *EXS* 2012, 101, 133-164.

(2) Singh, R.; Gautam, N.; Mishra, A.; Gupta, R. *Indian journal of pharmacology* 2011, 43, 246-253.

(3) Vallee, B. L.; Williams, R. J. *Proceedings of the National Academy of Sciences* 1968, 59, 498-505.

(4) Karlin, K. D. *Science* 1993, 261, 701-708.

(5) Prohaska, J. R. *Physiological reviews* 1987, 67, 858-901.

(6) Markesbery, W. R.; Ehmann, W. D.; Alauddin, M.; Hossain, T. I. *Neurobiol Aging* 1984, 5, 19-28.

(7) Tandy, S.; Bossart, K.; Mueller, R.; Ritschel, J.; Hauser, L.; Schulin, R.; Nowack, B. *Environmental Science & Technology* 2004, 38, 937-944.

(8) Fu, F.; Wang, Q. *Journal of environmental management* 2011, 92, 407-418.

(9) Liphadzi, M. S.; Kirkham, M. B.; Musil, C. F. *South African Journal of Botany* 2005, 71, 24-37.

(10) Soylak, M.; Saracoglu, S.; Elci, L.; Dogan, M. *International Journal of Environmental Analytical Chemistry* 2002, 82, 225-231.

(11) Aragay, G.; Pons, J.; Merkoçi, A. *Chemical Reviews* 2011, 111, 3433-3458.

(12) Li, Y.; Zhu, Z.; Zheng, H.; Jin, L.; Hu, S. *Journal of Analytical Atomic Spectrometry* 2016, 31, 383-389.

(13) Achterberg, E. P.; Braungardt, C. *Analytica Chimica Acta* 1999, 400, 381-397.

(14) Sonthalia, P.; McGaw, E.; Show, Y.; Swain, G. M. *Analytica Chimica Acta* 2004, 522, 35-44.

(15) Gillain, G. *Talanta* 1982, 29, 651-654.

(16) Feinberg, J. S.; Bowyer, W. J. *Microchemical Journal* 1993, 47, 72-78.

(17) Wang, J.; Lu, J.; Hocevar, S. B.; Farias, P. A.; Ogorevc, B. *Analytical chemistry* 2000, 72, 3218-3222.

(18) Kefala, G.; Economou, A.; Voulgaropoulos, A.; Sofoniou, M. *Talanta* 2003, 61, 603-610.

(19) March, G.; Nguyen, T. D.; Piro, B. *Biosensors* 2015, 5, 241-275.

(20) Meyerhoff, M. E.; Opdycke, W. N. *Advances in clinical chemistry* 1986, 25, 1-47.

(21) Li, T.-K.; Piechocki, J. T. *Clinical chemistry* 1971, 17, 411-416.

(22) Carlini, W. G.; Ransom, B. R. In Neurophysiological Techniques: Basic Methods and Concepts, Boulton, A. A.; Baker, G. B.; Vanderwolf, C. H., Eds.; Humana Press: Totowa, NJ, 1990, pp 227-320.

(23) Stamford, J. A.; Kruk, Z. L.; Millar, J. *Brain research* 1984, 299, 289-295.

(24) Howell, J. O.; Kuhr, W. G.; Ensman, R. E.; Mark Wightman, R. *Journal of Electroanalytical Chemistry and Interfacial Electrochemistry* 1986, 209, 77-90.

(25) Ponchon, J. L.; Cespuglio, R.; Gonon, F.; Jouvet, M.; Pujol, J. F. *Analytical chemistry* 1979, 51, 1483-1486.

(26) Armstrong-James, M.; Millar, J. *J Neurosci Methods* 1979, 1, 279-287.

(27) Bath, B. D.; Michael, D. J.; Trafton, B. J.; Joseph, J. D.; Runnels, P. L.; Wightman, R. M. *Analytical chemistry* 2000, 72, 5994-6002.

(28) Peters, J. L.; Miner, L. H.; Michael, A. C.; Sesack, S. R. *J Neurosci Meth* 2004, 137, 9-23.

(29) Pathirathna, P.; Yang, Y.; Forzley, K.; McElmurry, S. P.; Hashemi, P. *Analytical chemistry* 2012, 84, 6298-6302.

(30) Yang, Y.; Pathirathna, P.; Siriwardhane, T.; McElmurry, S. P.; Hashemi, P. *Analytical chemistry* 2013, 85, 7535-7541.

(31) Atcherley, C. W.; Laude, N. D.; Parent, K. L.; Heien, M. L. *Langmuir* 2013, 29, 14885-14892.

CHAPTER 2

VOLTAMMETRIC CHARACTERIZATION OF Cu(II) COMPLEXATION IN REAL-TIME
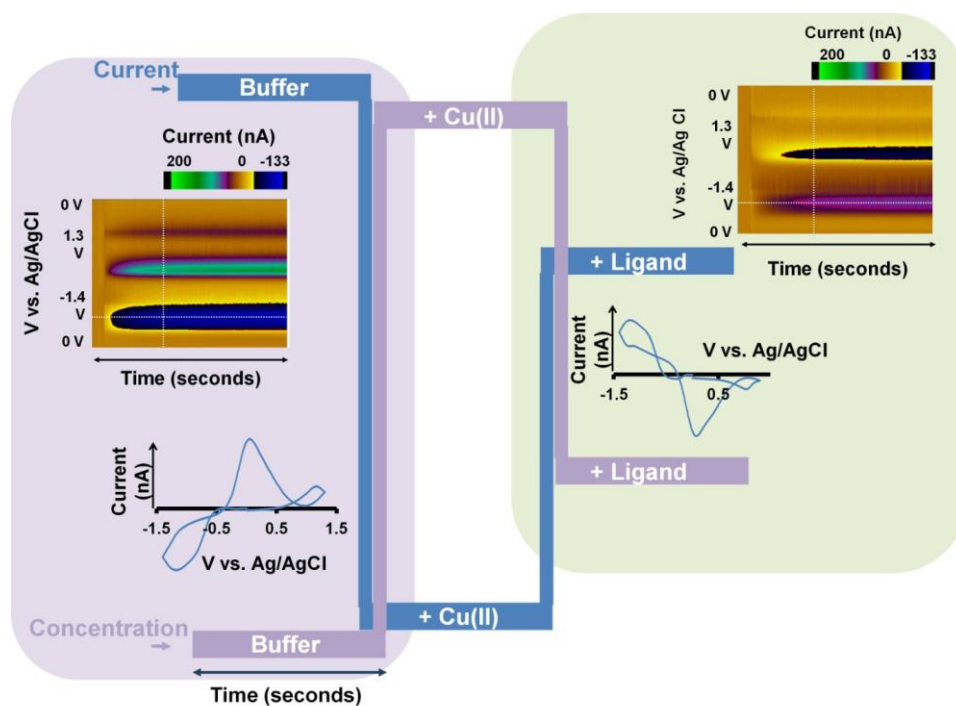
Siriwardhane, T.; Sulkanen, A.; Tremonti, A.; McElmurry, S. P.; Hashemi, P.: "Voltammetric Characterization of Cu(II) Complexation in Real Time"., Analytical Chemistry 2016 88 (15), 7603-7608. Reprinted with permission from Copyright(2016), American Chemical Society.

2.1 Abstract

Aqueous metal behavior is strongly regulated by speciation, which in turn is highly dependent on complexation. Trace metal complexation is difficult to characterize in dynamically changing systems due to a lack of analytical methods that can rapidly report free metal concentrations. In this paper, we perform proof of principle experiments that demonstrate the utility of fast-scan cyclic voltammetry for providing speciation information in real-time by characterizing dynamic Cu(II) binding. We study Cu(II) FSCV responses in 3-(N-morpholino)propanesulfonic acid (MOPS) buffer and characterize the hydrodynamic aspects of our experimental set-up (continuously stirred tank reactor). We observe Cu(II) complexation in real time using 5 ligands with differing formation constants of Cu(II) complexation. Finally, we utilize geochemical models to fit our real time experimental Cu(II)-binding curves. Our proof of principle experiments show that FSCV is a powerful tool for studying real time Cu(II) complexation, which is essential speciation information for better interpretation of Cu(II) behavior in dynamically changing systems, such as those encountered in biology or the environment.

2.2 Introduction

The behavior of trace metals in aqueous systems is controlled by speciation, which is dependent on a variety of factors including pH, temperature, and interactions with other substances (e.g., sorption and complexation).[1] Because of Cu(II)'s importance in biological, manufacturing and environmental

16

processes, there has been much emphasis on Cu(II) complexation.[2-4] The majority of previous work has looked at Cu(II) complexation in samples that are already complexed.[5] However, because Cu(II) complexation changes dynamically in the systems that we are interested in studying (environmental and biological),[6,7] it is desirable to us to monitor the concentration of this metal during complexation.

We recently described an electrochemical method, fast scan cyclic voltammetry (FSCV) at carbon-fiber microelectrodes (CFMs), for Cu(II) measurements in real-time.[8] Our method offers 100 ms temporal resolution and parts per trillion (ppt) limit of quantitation (LOQ). In this paper, we describe the application of FSCV to real-time Cu(II) binding. We first characterize some fundamental aspects of our experimental set-up including LOQ, media effects and electrode response as a function of solution convection. We then investigate Cu(II) binding with 5 different ligands encompassing a wide range of thermodynamic formation constants and demonstrate that Cu(II) complexation can be studied with FSCV in real time. The expected binding behavior of the ligands based on formation constants is mirrored by our experimental data. We utilize a geochemical model to fit our experimental curves which ultimately allows us to back-calculate formation constants that more accurately reflect our experimental setup. Our findings showcase FSCV's ability to assess Cu(II) binding in real-time, critical for future development of this tool as a speciation sensor in real systems.

2.3 Experimental section

2.3.1 Solutions

All solutions were at room temperature. A 0.005 M MOPS buffer was prepared using sodium chloride (0.00005 M, EMD Chemicals Inc, USA) and MOPS (Sigma Aldrich, USA). A stock solution of Cu(II) was prepared by dissolving copper nitrate ($Cu(NO_3)_2$) in 0.005 M MOPS buffer to reach a final concentration of 0.3 μM. The model ligands; ethylenediaminetetraacetic acid (EDTA) (Fisher Bioreagents, USA), citric acid (Sigma Aldrich, USA), glutamic acid (Sigma Aldrich, USA), 3-nitrosalicylic acid (3-NSA) (Sigma Aldrich, USA), and 5-nitrosalicylic acid (5-NSA) (Sigma Aldrich, USA) were prepared in 0.005 M MOPS buffer to reach a final concentration of 0.24 μM at pH 7.25.[9-11]

2.3.2 Carbon-fiber microelectrodes

A carbon-fiber of 5 μm radius (T-650, Cytec Industries, NJ) was vacuum-aspirated into a glass capillary (0.6 mm external diameter, 0.4 mm internal diameter, A-M Systems, Inc., Sequim, WA). A micropipette puller (Narishige, Tokyo, Japan) was used to form a carbon-glass seal under elevated temperature. The exposed carbon fiber was trimmed to make it approximately 150 μm long under a microscope.

2.3.3 Data acquisition and analysis

Waveform application, signal processing and data acquisition were performed with customized software, TH-1 (ESA, Chelmsford, MA) written in

LABVIEW (National Instruments, Austin, TX). A custom-built UEI potentiostat (University of North Carolina at Chapel Hill, Department of Chemistry Electronics Facility) was employed to control potential and current. A Cl$^-$ electroplated silver wire was used as the reference electrode and all the potential values were recorded with respect to this Ag/AgCl electrode. A Cu(II) specific waveform (-1.4 V to 1.3 V resting at 0 V with a scan rate of 600 Vs-1)[8] was applied to the electrode at 10 Hz. Data are presented with error bars representing the standard error of mean (SEM) and are analyzed with Student's paired t-tests.

2.3.4 Geochemical modelling

Solution chemistry was modeled using PHREEQCi (version 3.1.2, USGS), a thermodynamic based equilibrium modeling software commonly used to describe metal speciation.[12] To calculate the composition of solution species, PHREEQCi simultaneously balances equilibrium reactions describing pH, oxidation-reduction, complexation, gas dissolution, precipitation, etc. that are described in an associated program database. (One detailed output file of PHREEQCi analysis is shown in the supporting information). For this study, the database we used was a modified version of the MINTEQ.v4 database, originally developed by the U.S. Environmental Protection Agency,[13] that was updated to include protonation and complexation reactions for 3-NSA, 5-NSA and glutamic acid based on literature reported stability constants.[14,15] Mimicking experimental procedures, solutions were first modeled independently and then combined using the MIX routine in PHREEQCi. To account for hydrodynamics, an empirical equation was used to describe the fraction of solutions mixed over time.

Consistent with laboratory conditions, all solutions were modeled in equilibrium with $CO_2(g)$ ($10^{-3.392}$ atm) and $O_2(g)$ ($10^{-0.67}$ atm).[16] The pH of the solutions (buffer, copper nitrate, ligands, and mixtures) was found to be within 0.2 pH units of those predicted.

2.4 Results and discussion

2.4.1 Limit of quantitation

Trace metal concentrations are typically very low in real systems. Thus, a successful analysis method must have a LOQ within an appropriate concentration range. In environmental and biological systems, Cu(II) levels are in the parts per million and billion respectively.[17,18] It is straightforward to define the LOQ for analysis methods that measure total Cu(II), however LOQ is more challenging to define using our method that measures only free Cu(II). This is because free Cu(II) is inherently dependent on its matrix. For example, if calibrations are performed in a matrix that has affinity for Cu(II), a higher than actual LOQ might be encountered since the concentration of Cu(II) added to standards does not reflect the, now lower, free Cu(II) concentration. Further complicating this issue is a Cu(II) - CFM adsorption equilibrium that drives the FSCV response.[19] We showed that this equilibrium competes with solution equilibria, preconcentrating Cu(II) on the CFM surface and giving higher FSCV responses than can be predicted by calculating free Cu(II) with geochemical models. Therefore, to get as close to an accurate LOQ for our method, we performed a calibration in NaCl. Although NaCl has binding affinity for Cu(II), it is

very low (the range of different Cu(II)-chloride complexation Ks values are log K

= -2.29 – 0.2).[15] Figure 2.1 shows cathodic current extracted from fast scan cyclic

voltammograms after additions of Cu(II) in NaCl at different concentrations to

NaCl (0.005 M).

We used PHREEQCi, a geochemical speciation modeling tool, as

described previously,[20] to calculate the concentrations of free Cu(II) in our NaCl

calibration solutions where approximately 99% of Cu(II) is unbound. With this

measure, we report our LOQ as 620 ppt, which is sufficient for biological and

environmental applications where Cu(II) concentrations are typically much

higher.
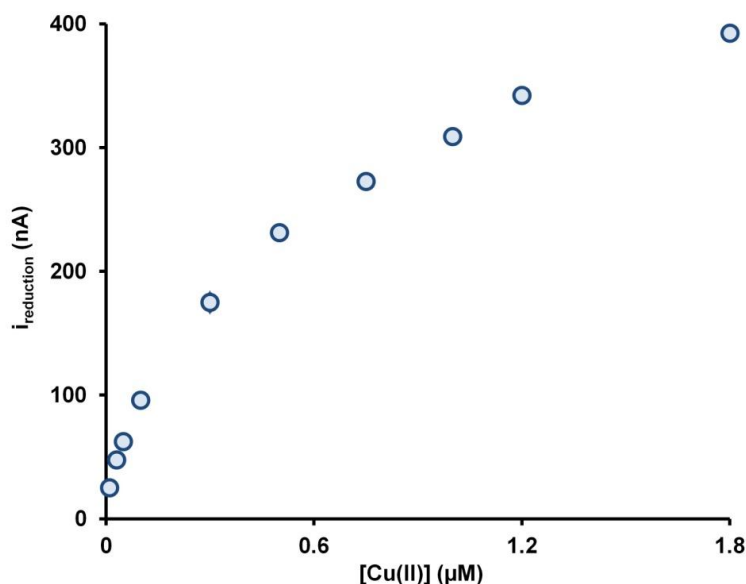
Figure 2.1. FSCV current responses for injection of different concentrations of Cu(II) dissolved in NaCl into a stirring solution of NaCl (small error bars are not visible under markers ranging from 1.2 – 8.1 nA).

This experiment explicitly demonstrates that matrix selection, specifically the use of matrices that do not bind Cu(II), is critical for laboratory characterizations.

2.4.2 Cu(II) characterization in mops buffer

For most laboratory analysis, it is often necessary to fix the pH of the test solution. However, the most common laboratory buffers (Tris, HEPES, Pipes etc.) have considerable metal binding capacity[21-23] which, as mentioned above, makes analysis challenging. In the past, we accounted for this using a post-hoc PHREEQCi analysis.[19,20] However, in this study we are interested in proof of principle experiments that show FSCV can evaluate Cu(II)-ligand binding in real-time. Having multiple competing equilibria greatly complicates such an evaluation; therefore, we aimed to employ a buffer solution with negligible metal binding capacity. In 2003, Mash et al. reported that MOPS buffer does not bind Cu(II) and is thus an excellent laboratory test solution for Cu(II) analysis.[22] To assess Cu(II) behavior in MOPS, we separately compared FSCV responses of Cu(II) injections (0.3 µM) into two constantly stirred solutions, NaCl (0.005 M) and MOPS buffer (0.005 M). Figure 2.2A shows that the Cu(II) response in NaCl is 179.7 ± 7.1 nA (n=7 ± SEM); while in MOPS the response is 160.5 ± 2.3 (n=7 ± SEM). Therefore, the Cu(II) response in MOPS is significantly decreased (p=0.02) despite the reported inability of MOPS binding Cu(II).

To establish whether or not MOPS binds Cu(II), a CFM was placed in a constantly stirred solution of Cu(II) (0.3 µM) in NaCl (0.005 M) and MOPS (0.005 M) was added as shown in Figure 2.2B (blue bar indicates injection time and

artifact). We previously performed this experiment with EDTA[8] and repeat it below with various ligands with different Cu(II) binding capacity. As we show below, even ligands with weak Cu(II) binding capacity (~K=10^8) cause significant decrease in response. Here there was no change in response, strongly suggesting that MOPS does not bind Cu(II).
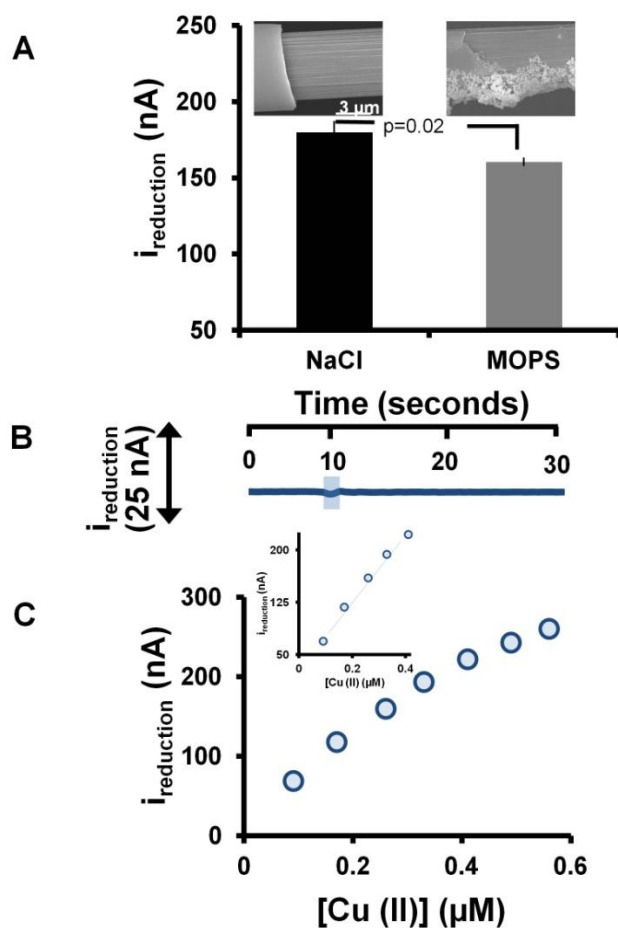
Figure 2.2. (A). Cu(II) (0.3 µM) responses in NaCl and MOPS. Scanning electron micrographs show electrodes after experimentation in NaCl and MOPS. (B). Current measurement during MOPS injection into Cu(II) (blue bar represents the injection time) (C). Cu(II) calibration in MOPS. Inset represents the linear range of the calibration curve.

Thus, to better understand the root of the electrode's decreased sensitivity towards Cu(II) in MOPS, we imaged the CFM at high resolution with scanning electron microscopy. Figure 2.2A (inset) compares an electrode after experimentation in NaCl medium with an electrode after experimentation in MOPS buffer. Substantial build-up is evident on the CFM that was exposed to MOPS, which likely accounts for the decline in Cu(II) response. Electrode fouling is not desirable for electrochemical analysis;[24] however fouling occurs rapidly and does not generally increase with time. The post-fouling sensitivity here for Cu(II) is still very high and sufficient for our characterizations.

Figure 2.2.C shows a Cu(II) calibration (n=9 ± SEM, the small error bars are not visible under markers ranging from 1.2 - 4.4 nA) in MOPS, the linear portion of which is utilized to convert current to Cu(II) concentration ([Cu(II)]) in the proceeding experiments. This calibration is very similar to the calibration in NaCl (Figure 2.1). We next characterized the electrode response in our experimental set-up.

2.4.3 Experimental characterization

The rapid addition of a Cu(II) spike to MOPS does not result in a step-change in the FSCV response. This phenomenon may be due to limited electrochemical kinetics or convection processes. It is unlikely that electrode kinetics is a limitation here because we previously showed square injection responses using flow injection analysis for Cu(II) and Pb.[8,20] Hence, a hydrodynamic characterization of the FSCV response was performed here. In

Figure 2.3, we rapidly injected a spike of Cu(II) (0.3 μM) into a continuously stirred-tank reactor (CSTR) of MOPS buffer stirring at 0, 200 and 500 rpm, as denoted by the yellow star.

The lower panel of Figure 2.3 shows representative FSCV color plots that arise upon spike addition of Cu(II) at different stir rates. The interpretation of color plots has previously been described.[25] In brief, potential is on the y-axis, time on the x-axis and current is in false color. Conversion of current taken from these color plots to Cu(II) concentration [Cu(II)] was also described previously.[8] Concisely, currents taken from the horizontal dashed lines (peak cathodic current) were converted to concentration via the calibration curve in Figure 2.2C.

We found that hydrodynamics significantly control the FSCV response. The effect of increasing the stir rate to 500 rpm was to produce the most rapid and high amplitude response as a higher steady-state rate of analyte is delivered to the electrode surface. Stirring speeds of more than 500 rpm were not feasible due to physical limitations of our prototype CSTR; therefore we utilized this mixing speed in our subsequent experiments.

The concentrations were averaged between 5 electrodes for each stir rate and displayed in the main graph in Figure 2.3. To account for the electrode response in terms of hydrodynamics, an empirical equation was derived to model the response, described by eq 2.1:

$$f_{mix} = ([0.0295 \ln(t) + 0.017] r_{bl}) / r_{std} \qquad \text{(eq 2.1)}$$

where the fraction mixed (f_{mix}) is a function of time (t) normalized by the baseline response (r_{bl}) and electrode response to the 0.3 µM Cu(II) spike (r_{std}). In Figure 2.3, the fit (blue dotted trace) can be used to describe the deviation from a theoretical step-change response due to mixing ($r^2 = 0.99$). In the proceeding complexation experiments, this fit will be used to account for hydrodynamic deviations from a step response.
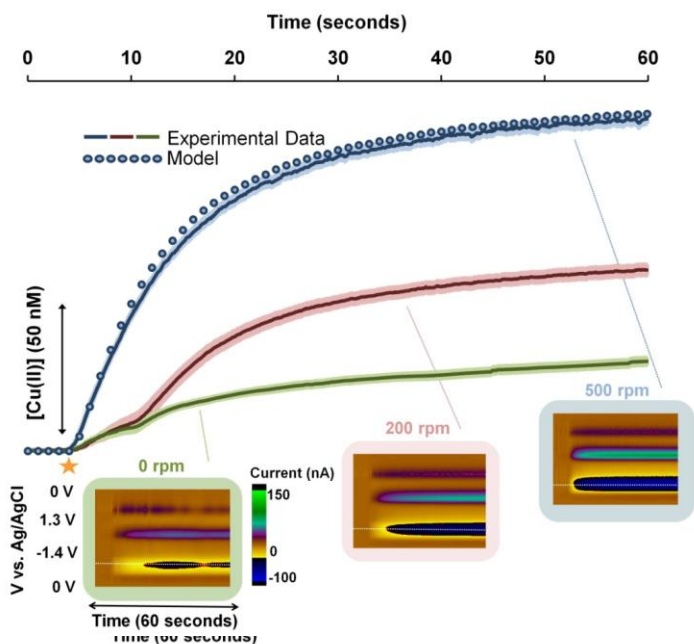
Figure 2.3. Cu(II) injections at different stir rates (0 rpm-green, 200 rpm-red, 500 rpm-blue) (n=5 electrodes ± SEM). Solid traces are experimental data. The blue dotted trace shows the empirical fit to the data using PHREEQCi.

2.4.4 Measurement of Cu(II) complexation in real-time

The experimental paradigm that we followed to investigate Cu(II) complexation is demonstrated via the illustrated schematic in Figure 2.4. FSCV is background subtracted to remove a large, non-Faradic current that arises because of higher scan rates employed. For background-subtraction to be

effective, files can be collected for a maximum of around 60 seconds while the background is stable. Because of this, our experimental paradigm is a two-step process. The first 60 second file is illustrated by the events in the purple box on the left. Here, a Cu(II) spike is added after 5 seconds to MOPS buffer stirred at 500 rpm. The color plot in this box is a representative example of a Cu(II) addition, the cyclic voltammogram (CV) taken from the vertical dashed line identifies Cu(II) via characteristic redox peaks.[8,19]
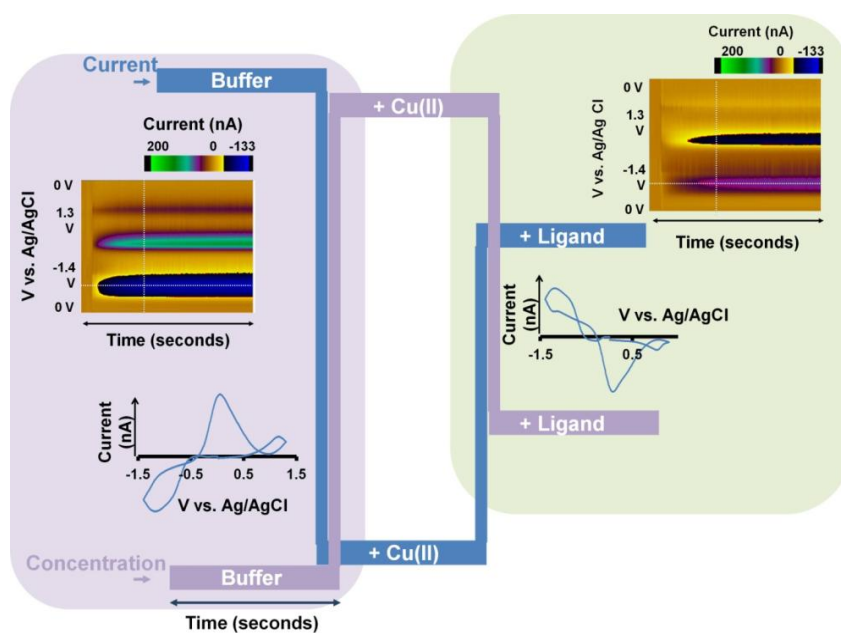
Figure 2.4. Two step Cu(II)-ligand complexation experimental paradigm. The change in the FSCV current is shown in blue. The color plot (left panel) represents the Cu injection and the characteristic CV for Cu(II) is below. Ligand addition is defined by the color plot (right panel) and the decrease in free Cu(II) in the solution is characterized by the inverse of the Cu(II) CV underneath.

Also in this box are the expected current and Cu(II) concentration ([Cu(II)]) traces after Cu(II) addition (current and concentration have an inverse relationship as previously described),[8] whereby an increase in reduction current corresponds to an increase in [Cu(II)].

In the second step, shown in the green box on the right, another file is taken for 60 seconds during which a ligand is added to the Cu(II)-MOPS solution after 5 seconds. The ligand is expected to complex Cu(II), resulting in a decrease in Cu(II) concentration. The color plot here is a representative example of ligand addition to Cu(II)-MOPS solution and the CV taken from the vertical dashed line is the inverse Cu(II) CV, showing that [Cu(II)] has indeed decreased, verifying complexation. Here, an increase in current corresponds to a decrease in [Cu(II)] as it is complexed by the ligand.

In applying this paradigm to real-time Cu(II) complexation, we deliberately chose 5 ligands to mimic the properties of ligands found naturally with Cu(II)-ligand complexation constants (K) ranging from $10^{8.1}$ to $10^{20.5}$. EDTA, citric acid and glutamic acid were chosen for their well-established thermodynamic characteristics, while two salicylic derivatives (3-NSA, 5-NSA) were intended to mimic humic acids, the major organic ligand found in environmental systems.[26] Furthermore, we were interested in evaluating the sensitivity of our method to these two derivatives of very similar formation constants.

Figure 2.5A shows an averaged Cu(II) injection into MOPS stirred at 500 rpm (n=5 injections onto 5 electrodes ± SEM) (blue solid) with the hydrodynamic fit superimposed on top (blue dots). Figure 2.5B is the result of addition of the five ligands at 80% Cu(II) concentration (5 injections onto 5 separate electrodes) to the Cu(II)-MOPS solution (solid purple, orange, teal, green and burgundy).

Each ligand caused the Cu(II) levels to drop as Cu(II) was complexed. As expected, the ligands with greater Cu(II) complexation/stability constant (K) resulted in greater decreases in Cu(II) levels. For example, 3-NSA (K=$10^{8.1}$) bound 0.0220 ± 0.001 μM (n=5 ± SEM) Cu(II), while 5-NSA (K=$10^{8.4}$) bound 0.0274 ±0.001 μM (n=5 ± SEM). This finding highlights an important strength of our method that even the smallest differences in K (i.e. $10^{8.1}$ vs. $10^{8.4}$) are mirrored by experimental data that shows 5-NSA binds more Cu(II) than 3-NSA.
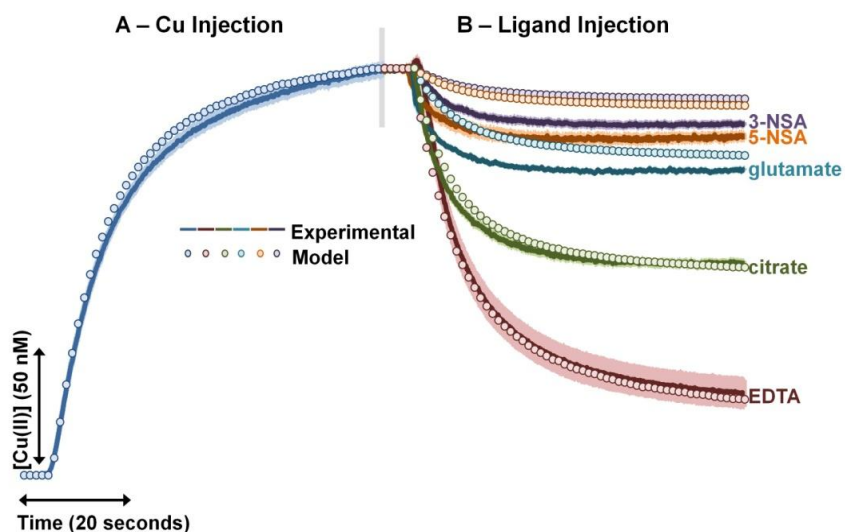
Figure 2.5. (A). The blue solid line shows the average Cu(II) injection into MOPS buffer. Blue dotted trace shows the hydrodynamic fit for the Cu(II) addition. (B). Decrease in [Cu(II)] after addition of ligands (step two), EDTA (burgundy), citrate (green), glutamate (teal), 5-NSA (orange), 3-NSA (purple) is shown by the solid lines. The corresponding dotted lines show modeled data.

glutamic (K=$10^{9.17}$) and citric acid (K=$10^{13.23}$) showed moderate Cu(II) binding of 0.0407 ± 0.001 μM and 0.0787 ± 0.001 μM (n=5 ± SEM), respectively. EDTA (K=$10^{20.5}$), a multidentate ligand, exhibited the greatest ability to bind Cu(II), a consequence of the high entropic and kinetic driving forces that favor

multidentate chelation. Here, 0.1307 ± 0.005 µM of Cu(II) (80% of Cu(II) in solution) was bound. While the information provided by this experiment is not novel in itself, we provide proof of principle, for the first time, that Cu(II) complexation can be studied at 100 ms, which is essentially real-time.

Our experimental data clearly correlates real-time Cu(II)-ligand binding to Ks. Next, we further verified that the experimental data accurately described Cu(II) complexation via PHREEQCi. Previously, we utilized this model to calculate free Pb and Cu(II) levels in our test solutions.[19,20,27] Based on reported Ks and our empirical fit using eq 3.1, here we utilize PHREEQCi to predict Cu binding after addition of the 5 ligands.

Using Equation 1, fractions of solutions were sequentially mixed. At each time-step, the model calculated new equilibrium conditions based on solution composition, which was then applied during the next mixing step. The purple, orange, teal, green and burgundy dots superimposed onto the solid lines describe model results. The model predictions closely align with [Cu(II)] observed during complexation with EDTA and citrate. Modeling results for the remaining 3 ligands are in the correct order (3-NSA>5-NSA>glutamate), however, appear to under-predict the extent of complexation observed in the experimental data. While the model accounts for changes in experimental conditions (e.g. ionic strength, pH), the literature Ks used for 5-NSA, 3-NSA and glutamate were determined under fundamentally different experimental conditions.[14,15] To obtain a more accurate K that reflects our experimental conditions, we utilized our model to back-predict K values. Because PHREEQCi balances numerous

chemical reactions during each time step, we opted to modify only a single K value for each ligand during this exercise. Since the pH remained fixed during experiments and was far from the acid dissociation (pKa) for each ligand, these parameters remained fixed.

Table 2.1. Reported stability constants used during modeling (Figure 2.3) and derived based on experimental results.

Ligand	Reaction	Log K (Literature)	Log K (Model)
3-nitrosalicylic acid	$Cu(II) + C_7H_3NO_5^{2-} \leftrightarrow CuC_7H_3NO_5$	8.1^{14}	8.35
5-nitrosalicylic acid	$Cu(II) + C_7H_3NO_5^{2-} \leftrightarrow CuC_7H_3NO_5$	8.3^{14}	8.61
glutamate	$Cu(II) + C_5H_7NO_4^{2-} \leftrightarrow CuC_5H_7NO_4$	9.17^{15}	9.165

Based on our experimental results, Ks for 3-NSA ($10^{8.35}$), 5-NSA ($10^{8.61}$) and glutamate ($10^{9.165}$) were able to be predicted (Table 3.1). This powerful

capability of our method to estimate Ks for unknown ligands provides evidence that FSCV can provide speciation information in real-time.

2.5 Conclusion

The behavior of metals in real systems is a function of speciation, in which complexation plays a major role. It is generally difficult to study trace metal complexation during rapid events. In this study using FSCV, we evaluated real-time Cu(II) complexation with a model set of ligands in MOPS buffer. We investigated the hydrodynamic profile of Cu(II) additions to a CSTR. By combining our hydrodynamic fits with PHREEQCi modeling, we closely modeled our experimental data and back-calculated complexation/stability constants for ligand interactions. FSCV is thus an important tool for characterizing Cu(II) speciation in real-time.

2.6 References

(1) Du Laing, G.; Rinklebe, J.; Vandecasteele, B.; Meers, E.; Tack, F. M. G. *Sci Total Environ* 2009, *407*, 3972-3985.

(2) Donnelly, P. S.; Xiao, Z.; Wedd, A. G. *Current Opinion in Chemical Biology* 2007, *11*, 128-133.

(3) Lu, X.; Wang, L.; Lei, K.; Huang, J.; Zhai, Y. *J Hazard Mater* 2009, *161*, 1058-1062.

(4) Hudson-Edwards, K. A.; Macklin, M. G.; Curtis, C. D.; Vaughan, D. J. *Environmental Science & Technology* 1996, *30*, 72-80.

(5) Malvankar, P. L.; Shinde, V. M. *Analyst* 1991, *116*, 1081-1084.

(6) Richarz, A.N.; Brätter, P. *Anal Bioanal Chem* 2002, *372*, 412-417.

(7) Morrison, M. A.; Benoit, G. *Journal of environmental quality* 2005, *34*, 1610-1619.

(8) Pathirathna, P.; Yang, Y.; Forzley, K.; McElmurry, S. P.; Hashemi, P. *Analytical chemistry* 2012, *84*, 6298-6302.

(9) Flash, P. *Journal of Chemical Education* 1994, *71*, A6.

(10) Aydin, R.; Ozer, U.; Turkel, N. *Turk. J. Chem.* 1997, *21*, 428-436.

(11) Potter, M. J.; Gilson, M. K.; McCammon, J. A. *Journal of the American Chemical Society* 1994, *116*, 10298-10299.

(12) Parkhurst, D. L.; and Appelo, C. A. J. Description of input and examples for PHREEQC version 3—A computer program for speciation, batch-reaction, one-dimensional transport, and inverse geochemical calculations: U.S. Geological Survey Techniques and Methods 2013, book 6, chap. A43, 497 p.

(13) Allison, J. D.; Brown, D. S.; Novo-Gradae, K. J. Environmental Research Laboratory, Office of Research and Development, U. S. Environmental Protection Agency: Athens, GA, 1990; 106 pages.

(14) Merce, A. L. R.; Mangrich, A. S.; Szpoganicz, B.; Levy, N. M.; Felcman, J. *Journal of the Brazilian Chemical Society* 1996, *7*, 239-245.

(15) Smith, R. M.; Martell, A. E.; Motekaitis, R. J.; NIST critically selected stability constants of metal complex database., Standard Reference Data Program, National Institute of Standards and Technology, U.S. Dept. of Commerce: Gaithersburg, MD, 2004.

(16) Aslamkhan, A. G.; Aslamkhan, A.; Ahearn, G. A. *The Journal of experimental zoology* 2002, *292*, 507-522.

(17) Flemming, C. A.; Trevors, J. T. *Water, Air, and Soil Pollution*, 1989, *44*, 143-158.

(18) Tchounwou, P. B.; Newsome, C.; Williams, J.; Glass, K. *Metal ions in biology and medicine* 2008, *10*, 285-290.

(19) Pathirathna, P.; Samaranayake, S.; Atcherley, C. W.; Parent, K. L.; Heien, M. L.; McElmurry, S. P.; Hashemi, P. *Analyst* 2014, *139*, 4673-4680.

(20) Yang, Y.; Pathirathna, P.; Siriwardhane, T.; McElmurry, S. P.; Hashemi, P. *Analytical chemistry* 2013, *85*, 7535-7541.

(21) McPhail, D. B.; Goodman, B. A. *Biochem J* 1984, *221*, 559-560.

(22) Mash, H. E.; Chin, Y. P.; Sigg, L.; Hari, R.; Xue, H. *Analytical chemistry* 2003, *75*, 671-677.

(23) Wyrzykowski, D.; Pilarski, B.; Jacewicz, D.; Chmurzyński, L. *J Therm Anal Calorim* 2013, *111*, 1829-1836.

(24) Manica, D. P.; Mitsumori, Y.; Ewing, A. G. *Analytical chemistry* 2003, *75*, 4572-4577.

(25) Michael, D.; Travis, E. R.; Wightman, R. M. *Analytical chemistry* 1998, *70*, 586A-592A.

(26) Kostic, I.; Andelkovic, T.; Nikolic, R., Bojic, A.; Purenovic, M.,; Blagojevic, S.; Andelkovic, D. *J. Serb. Chem. Soc* 2011, *76(9)*, 1325-1336.

(27) McElmurry, S. P.; Long, D. T.; Voice, T. C. *Applied Geochemistry* 2010, *25*, 650-660.

CHAPTER 3

FAST VOLTAMMETRY OF METALS AT CARBON-FIBER MICROELECTRODES: RAPID DETERMINATION OF SOLUTION FORMATION CONSTANTS

A predictive relationship between Cu(II) and model ligands were established to provide proof of principle that FSCV is capable of providing speciation information. I contributed both experimentally and intellectually and the results of this project directed me to contribute towards my next co-project.
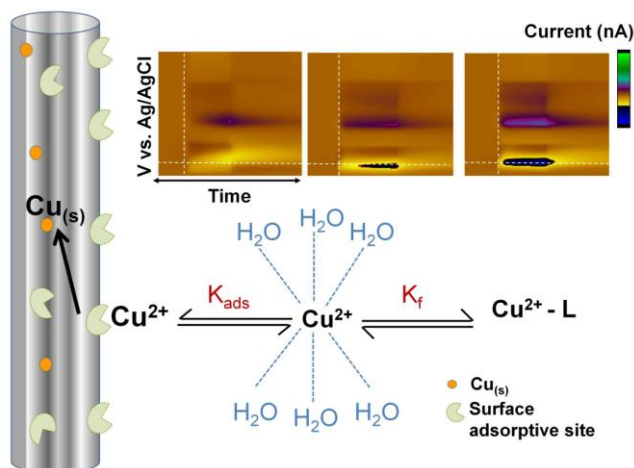
Pathirathna, P.; **Siriwardhane, T**.; Morgan S.L.; McElmurry, S. P.; Hashemi, P.; "Fast voltammetry of metals at carbon-fiber microelectrodes: rapid determination of solution formation constants"., Analyst 2016, 141, 6432 Reprinted with permission from Copyright(2016), Royal Chemical Society.

3.1 Abstract

Metal speciation controls the behavior of aqueous metal ions. Fundamental thermodynamic parameters, such as a formation constant (K_f) of metal-ligand equilibria provide useful speciation information. Although this information can be determined by spectroscopic techniques with high accuracy, it comes at the expense of time and cost. In this work, we studied Cu(II) complexation with different ligands using an ultra-fast method, fast scan cyclic voltammetry (FSCV) at carbon fiber microelectrodes (CFMs). We observed a correlation between FSCV response and previously reported Cu(II)-ligand equilibrium constants. This relationship allowed us to model a predictive relationship between K_f and 16 model ligands. We hence present an essential proof of principle study that highlight's FSCV's capability to prove speciation information in real time.

3.2 Introduction

Trace metals serve a variety roles in different fields, including scientific, biological, environmental, catalysis, manufacturing, and agricultural.[1-3] The behavior of metals is fundamentally dependent on speciation, to which complexation is a major contributor.[4-6] Thus, to better understand the mechanisms and impact of trace metals, it is desirable to define metal speciation *in situ* in delicate, dynamically changing, and often harsh systems.

Thermodynamic parameters, such as the formation constant of metal-ligand equilibria (K_f), provide an index of the relative strength of intervening complexation reactions in aqueous solution. While spectroscopic methods can

36

deliver this information with high accuracy, the secondary methods required are technically laborious and time consuming.[7,8] A rapid delivery of this parameter would provide key analytical information where there is a time demand.

We recently described real-time analysis of Cu(II) and Pb(II) using fast scan cyclic voltammetry (FSCV) at carbon fiber microelectrodes (CFMs).[9,10] We found that the endogenous adsorptive properties of an activated CFMs afford extreme sensitivity to the FSCV measurement.[11] We attributed the high sensitivity of the response to a CFM-Cu(II) adsorption equilibrium on the surface of the microelectrodes that competes with solution equilibria to shift towards more adsorbed Cu(II) on the CFM surface.[11] This phenomenon is not only auspicious in providing enhanced detection sensitivity but, as we explore in this paper, can also be exploited to provide rapid information about overall solution K_f.

Here using FSCV, we study Cu(II) complexation with a variety of model ligands that encompass a wide range of Cu(II)-ligand equilibrium constants. We took a non-linear least squares estimation approach to model a correlation between the Cu(II) FSCV response and Cu(II)-ligand formation constants. The model accurately captured our data (R^2=0.9776, standard deviation of residuals = 9.111 and no outliers). This strong correlation thereby provides an essential proof of principle study to showcase FSCV's versatility in providing not only chemical, but also speciation information in real-time. Our data represent an important first step towards a real-time speciation sensor.

3.3 Experimental Section

3.3.1 Solutions

All chemicals were purchased from Sigma-Aldrich (St. Louis, MO) unless otherwise specified. The source of Cu(II) was $Cu(NO_3)_2$. Ethylenedaminetetraacetic acid (EDTA), citric acid, 5-nitrosalicylic acid (5-NSA), 3-nitrosalicylic acid (3-NSA), salicylic acid , oxalic acid, glycine (GLY), dimethylglycine (DMG), nitrilotriacetic acid (NTA), salicylaldehyde, valine (VAL), 2-Ethylidene-1,5-dimethyl-3,3-diphenylpyrrolidine (EDDP), diethylenetriaminepentaacetic acid (DTPA), ethylene glycol-bis(2-aminoethylether)-N,N,N',N'-tetraacetic acid (EGTA), 3,4-dihydroxybenzoic acid (DBA), aspartic acid and glutamic acid served as the model ligands for Cu(II)-ligand complexation processes. The Cu(II)-ligand mixtures were prepared in 1:1 stoichiometric ratio in NaCl (0.01 M) prior to flow injection analysis (FIA) at ambient temperature and pressure. Each solution mixture was allowed sufficient time (>2 h) to come close to steady-state equilibrium prior to experimentation. The pH of each mixture was recorded, and incorporated into geochemical modeling performed using PHREEQCi.

3.3.2 Microelectrodes

CFMs were constructed as previously described.[9-11] In brief, a carbon fiber (5 µm radius, T-650, Cytec Industries, NJ) was aspirated into a glass capillary (0.6 mm external diameter, 0.4 mm internal diameter, A-M Systems, Inc., Sequim, WA) under vacuum suction. The carbon-glass seal was formed by pulling the fiber - filled capillary with a vertical micropipette puller (Narishige,

Tokyo, Japan) under gravity producing a tapered end. The pulled electrodes were cut to approximately 150 μm (for FSCV) or 30-40 μm (for fast scan controlled adsorption voltammetry (FSCAV)) under an optical microscope. Each experiment was repeated utilizing four electrodes with three replicates per electrodes.

3.3.3 Flow Injection Analysis

Flow injection analysis was performed in a system custom built in-house. CFMs were inserted to flangeless short 1/8 nuts (PEEK P-335, IDEX, Middleboro, MA) exposing a small portion of the tip (2 mm) outside of the nut. A HPLC union (Elbow PEEK 3432, IDEX, Middleboro, MA) was modified such that the nut containing microelectrode was fastened to one end. The out-flowing stream of the FIA buffer was fastened to the other end of the elbow union. Two holes were drilled into the union for the incorporation of the reference electrode and for the 'waste' flow stream. A syringe infusion pump (KD Scientific, Model KDS-410, Holliston, MA) was used to maintain the flow. The analyte was introduced into the flow stream for 10 seconds via a six-port HPLC loop injector (Rheodyne Model 7010 valve, VICI, Houston, TX) as a rectangular pulse.

3.3.4 Fast Scan Cyclic Voltammetry

A potentiostat (Dagan Corporation, Minneapolis, MN, USA) and a custom-built breakout box, incorporating national instruments data acquisition cards, for potential and filter application, and current transduction were employed in FSCV experiments. Data collection, data analysis with background subtraction and signal averaging and digital filtration were performed with custom built software

(Knowmad Technologies LLC, Tucson, AZ). All voltammetric experiments engaged a 2-electrode system. The combined counter/reference electrode was a Ag/AgCl electrode constructed by plating Cl- ions on a Ag wire. An optimized Cu(II)- waveform (-1.0 V – +1.3 V at 100 Hz, resting potential of 0 V, at 600 V s^{-1}) was applied to collect cyclic voltammograms (CVs).

3.3.5 Solution Chemistry

PHREEQCi, a geochemical modelling software (available for free at http://wwwbrr.cr.usgs.gov/projects/GWC_coupled/phreeqc/) was employed to predict the solution chemistry of Cu(II)-ligand mixtures in NaCl as previously reported.[11] Equilibrium constants required to anticipate the speciation of each of the ligand mixtures were based on the MINTEQ.v4 database developed by the U.S. Environmental Protection Agency[12] he additional constants for complexation with solutions were modelled in equilibrium with CO_2(g) ($10^{-4.8}$ atm.) and $O_{2(g)}$ ($10^{-0.67}$ atm.).[13]

3.3.6 Fast Scan Controlled-Adsorption Voltammetry (FSCAV)

FSCAV experiments were performed as described elsewhere.[14] Briefly, an electronic relay (ADG-419, Analogue Devices) was used to switch between the applied waveform (-1.0 V – +1.3 V at 100 Hz, resting potential of 0 V, at 600 V s^{-1}) and a constant potential of 0 V for 10 seconds, to a CFM placed in a Cu(II)-ligand solution. The constant potential adsorption period was 10 seconds. The analysis for total adsorbed copper was performed using the first background-subtracted copper cyclic voltammogram with in house LabVIEW 2012 software by integrating the reduction peak. Faraday's law was used to convert total charge

to a surface concentration (ΓCu), and the linearized Langmuir isotherm was used to fit the measured data (eq. 4.1) where C is the [Cu(II)] in bulk solution, Γmax is the maximum monolayer surface coverage, and K is the equilibrium constant for adsorption.

$$C/\Gamma_{Cu} = (1/\Gamma_{Max})C + 1/(\Gamma_{Max} K) \qquad\qquad (eq.3.1)$$

3.3.7 Modeling and Statistical Analysis

The Curve Fitting Toolbox in Matlab®(Natick, MA) was used for nonlinear weighted least squares estimation of the parameters of the model, y = a x-b. In this model, x represents calculated values of $\log_{10}(K_f)$, and y is the cathodic current measured for each ligand analyzed. Robust fitting was performed using the bisquare weighting option, along with the Levenberg-Marquardt algorithm to minimize a weighted sum of squares of residuals by iterated re-weighted least squares.[15-18] This approach assigns weights to data in proportion to the distance from each point to the fitted line: data closer to the fitted model have high weights, points far from the model have lower weights, and finally, data that are further from the fitted model than could be expected by chance are assigned zero weight.

3.4 Results and Discussion

3.4.1 Effect of Mass Transport Rate and Waveform Application Frequency on FSCV Response

The CFMs utilized in this study have a cylindrical geometry and sit in a hemispherical diffusion field within the FIA flow cell. Mass transport of Cu(II) to the electrode surface occurs primarily via convection and diffusion. Since we

previously observed a higher FSCV sensitivity to Cu(II) than expected from the levels of free, unbound Cu(II) in Tris buffer,[11] we hypothesize that the CFM-Cu(II) adsorption equilibrium might yield a predictive relationship between Kf and FSCV response. However there are fundamental experimental parameters of our system, namely waveform application frequency and rate of mass transport that affect the CFM-Cu(II) equilibrium, that need to be addressed before focusing on our hypothesis.

In the FIA system utilized, flow follows a well-defined laminar profile thus the rate of mass transport can be controlled by varying the flow rate of the FIA system. Our prior experiments and the experiments in this chapter are at a flow rate of 2 mL min^{-1}, consistent with other literature reports.[19] In Figure 3.1 (left segment) are displayed maximum cathodic FSCV currents (i_c) of FIA of a 1:1 stoichiometric ratio of Cu(II)-EDTA with systematic increase of flow rate from 0.5 mL min^{-1} to 8 mL min^{-1}. As expected, a higher FSCV response is concomitant with increased flow because of increased rate of mass transport. The highest response (98.2 ± 1 nA) was found at our routine flow rate of 2 mL min^{-1}, after which the response began to decrease likely due to physical limitations of our flow cell (pressure limit).

We next addressed how the waveform application frequency affects FSCV response. The same analyte was injected into a flow stream at 2 mL min^{-1} while waveform application frequency was varied from 1 Hz to 50 Hz. The hypothesis here was that by increasing application frequency, adsorption time becomes limited resulting in lower surface adsorbed Cu(II) and hence a lower FSCV

response. This phenomenon has previously been observed for neurotransmitters[14, 20] and is consistent for Cu(II) as shown in the right segment of Figure 3.1 where maximum current was observed for lower application frequencies. However, because this increase in signal comes at the expense of the temporal resolution, we chose to maintain 10 Hz as our FSCV waveform application frequency since sensitivity is sufficient for analysis.
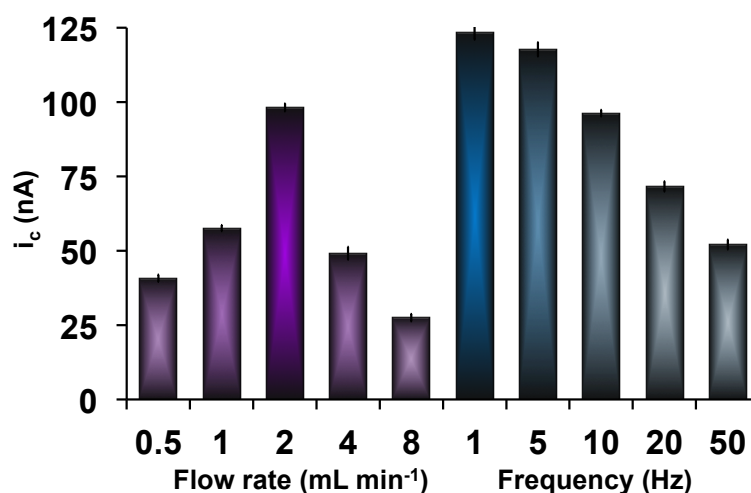
Figure 3.1 Left: Maximum cathodic current (i_c) for Cu(II) voltammograms obtained from Cu(II)- EDTA mixture at a flow rate of 0.5, 1, 2, 4, and 8 mL min^{-1}. Right: Maximum cathodic current for Cu(II) voltammograms obtained from Cu(II)- EDTA mixture in FIA system at frequencies of 1, 5, 10, 20, and 50 Hz.

This experiment shows that both mass transport rate and waveform application frequency affect the FSCV response because of different Cu(II) adsorption profiles on the CFM surface. Importantly, the high reproducibility of the response per parameter (small error bars on Figure 3.1) shows that with a given set of parameters, Cu(II) adsorption is consistent. This allows us to

confidently set the flow rate and waveform application frequency for the remaining experiments in this paper at 2 mL min^{-1} and 10 Hz respectively, providing experimental accuracy in the following Cu(II)-ligand comparison studies.

3.4.2 FSCV Response, Free Cu and Computationally Derived Ks

We previously noted higher than the expected FSCV sensitivity towards Cu(II) in a solution of Tris buffer where approximately 98% of Cu(II) was bound.[11] We sought to observe whether this phenomenon holds in other Cu(II) binding media. Solutions were made with differing degrees of Cu(II) binding ability, indicated by K_f for Cu(II)-ligand complexation. Those were 1:1 mixtures of Cu and EDTA (log K_f = 20.3), citric acid (log K_f = 13.2), and 5-NSA (log K_f = 8.3) in NaCl. We performed FSCV on each solution and present the raw data in the color plots in Figure 3.2A. The maximum cathodic current from the cyclic voltammograms extracted from the color plots is shown in the table in Figure 3.2B. These data follow our previous observation with Tris buffer[11] and are a consequence of a fundamental difference between FSCV and classical cyclic voltammetry. That is, while traditional voltammetry is heavily diffusion driven, the FSCV response is primarily driven by analyte adsorption to the carbon surface. We hypothesize that the CFM-Cu(II)equilibrium shifts, according to Le Chatelier's principle, towards the left as depicted in Figure 3.2B below, resulting in higher than expected (from a pure solution chemistry perspective) FSCV signal. We illustrate this effect further, by using a geochemical speciation model, PHREEQCi, to predict the % free [Cu(II)] in each of the Cu(II) -ligand mixtures, which is also presented in the

table in Figure 3.2B. In all cases, the Cu(II) equilibrium shifted towards the CFM; it is of particular note that, even with the EDTA complex, where only 0.02% Cu is unbound, there is appreciable FSCV signal (208.9 ± 4 nA). Furthermore, there is an apparent relationship between FSCV response and K_f.
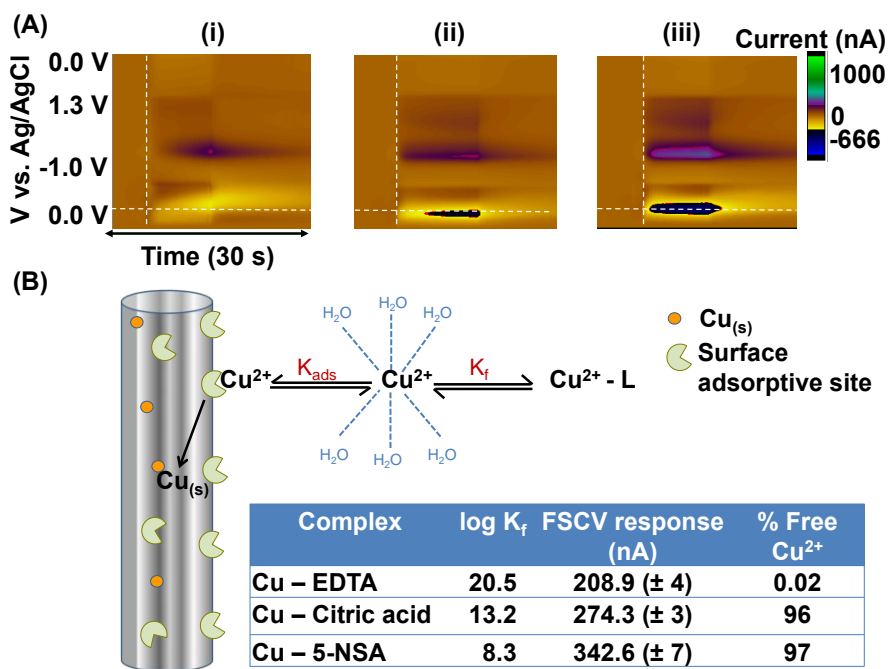
Figure 3.2 (A): Representative color plots obtained after injection of (i) Cu(II) -EDTA, (ii) Cu(II)-citric acid and (iii) Cu(II)-5-NSA complexes into FIA system. White horizontal dashed line indicates the Cu(II) electroreduction vs. Ag/AgCl electrode. White vertical dashed lines indicate injection time. (B): Schematic illustrating Cu(II)- CFM and Cu(II)-ligand equilibria in aqueous solution.

These experiments strongly support our postulation that the CFM- Cu(II) adsorption pulls Cu(II) through the associated aqueous phase equilibrium resulting in an increase in signal, and we next seek to find whether this relationship is predictable. However, before this data can be used for predictive

modeling, it is critical to show that the CFM-Cu(II) adsorption equilibrium is consistent between media.

3.4.3 Adsorption Isotherms

By constructing adsorption isotherms, we can calculate the equilibrium constant (K_{ads}) accompanying CFM-Cu(II) monolayer adsorption. We previously created such isotherms for Cu(II) in NaCl and Tris buffer[14, 21] and we followed the same procedure here. Figure 3.3 shows the Langmuir fits to the adsorption isotherms with two x-axes. These axes represent the concentration of Cu(II) added to solution $[Cu(II)]_A$ and the level of unbound Cu(II) as predicted with PHREEQCi $[Cu(II)]_B$. As expected the difference between the two x-value series is highest in the presence of EDTA for the Cu(II)-EDTA solution, since only 0.02% Cu(II) is free whereas citric acid and 5-NSA leave 96-97% Cu(II) unbound. K_B is the K_{ads} calculated via $[Cu(II)]_B$ and shows good agreement between the 3 ligands and with the K_{ads} that we previously reported for Cu(II) -NaCl (4.05×10^9) and Cu(II)-Tris (4.43×10^9) mixtures[21].

This experiment verifies that Cu(II) monolayer adsorption is not restricted or promoted significantly by the surrounding matrix and allows us to pursue whether a predictive relationship exists between the FSCV response and solution K_f.

3.4.4 Predictive Relationship Between Solution K_f and FSCV response

K_f expresses the relative strength of the interaction between two species. Determination of K_f values, particularly for metals, are essential to different

applications including chelation therapy,[22-24] MRI contrast production processes,[25, 26] and the ion selective electrode manufacturing processes.[27] Moreover, K_f values allow the calculation of thermodynamic properties like entropy and enthalpy, providing additional significant information of interest.
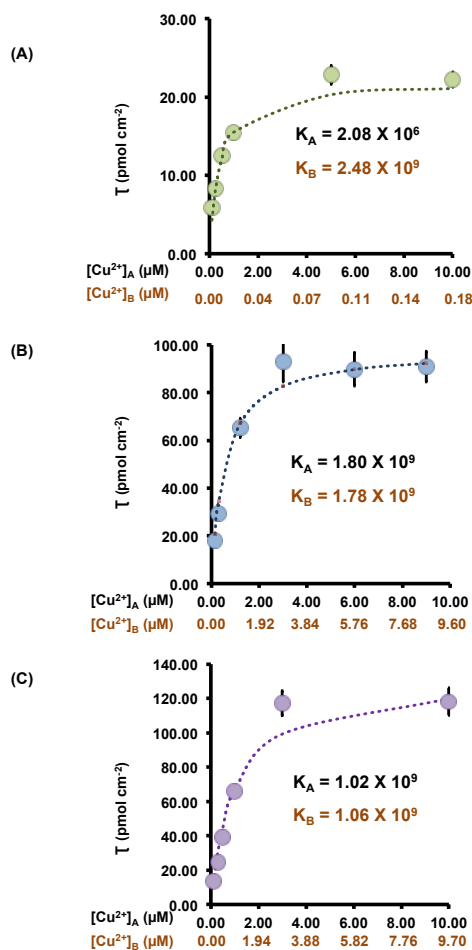
Figure 3.3: Langmuir adsorption isotherms (A) Cu(II)-EDTA (B) Cu(II)-citric acid and (C) Cu(II)-5-NSA mixtures in NaCl. [Cu(II)]$_A$ represents the added [Cu(II)] and [Cu(II)]$_B$ represents the free [Cu(II)] calculated from PHREEQCi. K_A and K_B are equilibrium constants for Cu(II) adsorption onto CFM with respect to [Cu(II)]$_A$ and [Cu(II)]$_B$.

Because of the wide interest in determining solution K_f, the precision and accuracy of traditional K_f measurements has been greatly enhanced from the first

method introduced by Jannik Bjerrum,[28] although the principle of the method remains the same. In brief, an acidic solution of a protonated ligand and metal is titrated and the activity or the concentration of hydrogen ions is measured with a glass electrode.

However, glass electrodes fail to monitor some reactions and alternative procedures become necessary. These alternate methods include spectroscopic techniques such as absorption, fluorescence and NMR spectroscopy.[29-31] Although glass electrodes and spectroscopic techniques[7,8] provide sensitive and accurate information, these procedures are offline, lengthy and can be laborious. If we were to find a predictive relationship between FSCV response and K_f, we could report solution K_f using our inexpensive CFMs with a simple flow injection system with the ultra-fast temporal resolution of FSCV.
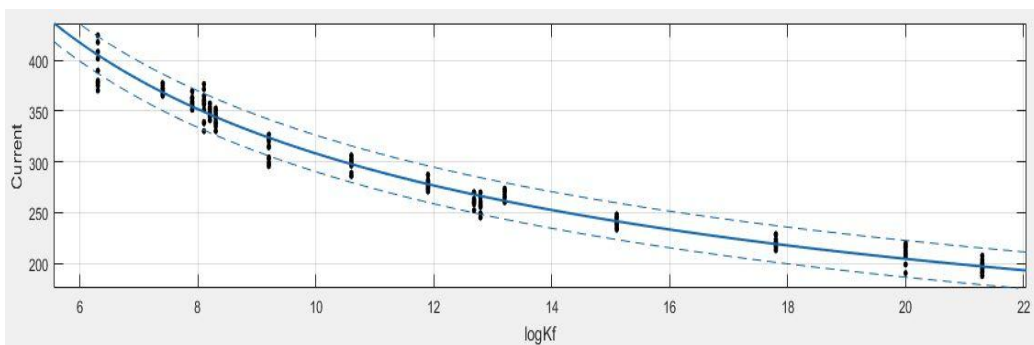
Figure 3.4: The correlation between FSCV current and log Kf for 16 different Cu(II)-ligand complexes. The ligands are (A) oxalic acid (B) salicylaldehyde (C) VAL (D) 3-NSA (E) GLY (F) 5-NSA (G) glutamic acid (H) salicylic acid (I) DMG (J) NTA (K) DBA (L) citric acid, (M) EDDP (N) EGTA (O) EDTA and (P) DTPA.

As proof of principle that FSCV can achieve this type of measurement, we employed 16 different ligands and created mixtures with Cu(II) in the same

manner described earlier; EDTA, citric acid, 5-NSA, 3-NSA, salicylic acid, oxalic acid, GLY, DMG, NTA, salicylaldehyde, VAL, EDDP,DTPA, EGTA, DBA and glutamic acid served as the model ligands. Cu(II)- ligand mixtures were analyzed with FIA using FSCV and the relationship between cathodic current and log K_f [32,33] was modelled as shown in Figure 3.4, in which replicate current data for each ligand are indicated by black dots, and the fitted model and its 95% confidence intervals by the solid blue curve and dashed lines.

The robust fit algorithm employed uses iteratively reweighted least squares with a bisquare weighting function.[16,17] This algorithm estimates parameters that are approximately 95% statistically efficient as ordinary least squares estimates, as long as the measured responses are normally distributed and without outliers. Goodness of fit statistics for the fitted model were excellent: the coefficient of determination (R^2) and adjusted R^2 values were 0.9776 and 0.9775, respectively; the standard deviation of residuals (root mean square error) was 9.111, and no outliers were detected. The estimated values (and 95% confidence intervals) for the parameters of the exponential model, $y = ax^b$, were: a = 1207 (1171, 1244), and b = -0.5929 (-0.6062, -0.5796). This model enables determination of ligand K_f values via FSCV measurements in a rapid laboratory setting, and offers simplification of speciation analysis in comparison to current capabilities.

Furthermore, we used this model to predict the log K_f of aspartic acid by using the observed FSCV response for Cu(II) - aspartic acid mixture as the y component. Agreeably, our model yields log K_f as 8.63, which closely agrees well

with previously reported values.[32] An important caveat here is that this model can only currently function when the $[Cu(II)]_{added}$ is a known (in this case, the same) value. In our future work, we are working to incorporate an ambient $[Cu(II)]$ measurement that would afford speciation information in authentic samples of unknown Cu(II) concentration. Nonetheless, we present here an important laboratory tool for ultra rapid delivery of speciation information.

3.5 Conclusions

Copper-ligand complexation equilibria can be studied at high time resolution with FSCV. In this work, we observed a strong relationship between FSCV response for different Cu(II)-ligand solutions and their corresponding equilibrium constants. This study is proof of principle that FSCV can be utilized to study speciation on rapid time scales.

3.6 References

(1) Larsson, P. F.; Correa, A.; Carril, M.; Norrby, P. O.; Bolm, C. *Angewandte Chemie International Edition* 2009, 48, 5691-5693.

(2) Luoma, S. N.; Rainbow, P. S.; Luoma, S. Metal Contamination in Aquatic Environments: Science and Lateral Management; Cambridge University Press, 2008.

(3) He, Z. L.; Yang, X. E.; Stoffella, P. J. *Journal of Trace Elements in Medicine and Biology* 2005, 19, 125-140.

(4) Allen, H. E.; Hansen, D. J. *Water Environment Research* 1996, 68, 42-54.

(5) Pagenkopf, G. K.; Russo, R. C.; Thurston, R. V. *Journal of the Fisheries Board of Canada* 1974, 31, 462-465.

(6) Sunda, W. The relationship between cupric ion activity and the toxicity of copper to phytoplankton. Massachusetts Institute of Technology and Woods Hole Oceanographic Institution 1975.

(7) Nagaj, J.; Stokowa-Sołtys, K.; Kurowska, E.; Frączyk, T.; Jeżowska-Bojczuk, M.; Bal, W. *Inorganic Chemistry* 2013, 52, 13927-13933.

(8) Hirose, K. *Journal of Inclusion Phenomena and Macrocyclic Chemistry* 2001, 39, 193-209.

(9) Pathirathna, P.; Yang, Y.; Forzley, K.; McElmurry, S. P.; Hashemi, P. *Analytical Chemistry* 2012, 84, 6298-6302.

(10) Yang, Y.; Pathirathna, P.; Siriwardhane, T.; McElmurry, S. P.; Hashemi, P. *Analytical Chemistry* 2013, 85, 7535-7541.

(11) Pathirathna, P.; Samaranayake, S.; Atcherley, C. W.; Parent, K. L.; Heien, M. L.; McElmurry, S. P.; Hashemi, P. *The Analyst* 2014.

(12) Allison, J. D., Brown, D.S.,Novo-Gradac, K.J. MINTEQA2/PRODEFA2--A Geochemical Assessment Model for EnvironmentalSystems--version 3.0 User's Manual,Environmental Research Laboratory, Office of Research and Development, U.S. Environmental Protection Agency 1990, 106.

(13) Aslamkhan, A. G.; Aslamkhan, A.; Ahearn, G. A. *Journal of Experimental Zoology* 2002, 292, 507-522.

(14) Atcherley, C. W.; Laude, N. D.; Parent, K. L.; Heien, M. L. *Langmuir* 2013, 29, 14885-14892.

(15) Huber, P.; Ronchetti, E. *Robust Statistics*; John Wiley, 2009.

(16) Huber, P. J. *Robust Statistics* 1981, 199-242.

(17) Holland, P. W.; Welsch, R. E. *Communications in Statistics-theory and Methods* 1977, 6, 813-827.

(18) Fox, J. *Applied Regression Analysis, Linear Models, and Related Methods; Sage Publications, Inc,* 1997.

(19) Hashemi, P.; Dankoski, E. C.; Petrovic, J.; Keithley, R. B.; Wightman, R. *Analytical Chemistry* 2009, 81, 9462-9471.

(20) Jacobs, C. B.; Ivanov, I. N.; Nguyen, M. D.; Zestos, A. G.; Venton, B. J. *Analytical Chemistry* 2014, 86, 5721-5727.

(21) Pathirathna, P.; Samaranayake, S.; Atcherley, C. W.; Parent, K. L.; Heien, M. L.; McElmurry, S. P.; Hashemi, P. *The Analyst* 2014, 139, 4673-4680.

(22) House, E.; Collingwood, J.; Khan, A.; Korchazkina, O.; Berthon, G.; Exley, C. *Journal of Alzheimer's disease*: JAD 2004, 6, 291-301.

(23) Barry, M.; Flynn, D. M.; Letsky, E. A.; Risdon, R. *BMJ* 1974, 2, 16-20.

(24) Flora, S.; Mittal, M.; Mehta, A. *Indian Journal of Medical Research* 2008, 128, 501.

(25) Caravan, P.; Ellison, J. J.; McMurry, T. J.; Lauffer, R. B. *Chemical Reviews* 1999, 99, 2293-2352.

(26) Werner, E. J.; Datta, A.; Jocher, C. J.; Raymond, K. N. *Angewandte Chemie International Edition* 2008, 47, 8568-8580.

(27) Morf, W. E. The Principles of Ion-selective Electrodes and of Membrane Transport; *Elsevier,* 2012.

(28) Bjerrum, J.; Andersen, P. Metal Ammine Formation in Aqueous Solution; Munksgaard, 1945.

(29) Gans, P.; Sabatini, A.; Vacca, A. *Talanta* 1996, 43, 1739-1753.

(30) Frensdorff, H. K. *Journal of the American Chemical Society* 1971, 93, 600-606.

(31) Wimmer, R.; Aachmann, F. L.; Larsen, K. L.; Petersen, S. B. *Carbohyd Res* 2002, 337, 841-849.

(32) Furia, T. E. CRC Handbook of Food Additives; CRC press, 1973; Vol. 1.

(33) Analytical and Biological Products Catalog 2012, Dojindo Molecular Technologies, Inc.,Washington, D.C. 252-253.

CHAPTER 4

FAST VOLTAMMETRY OF METALS AT CARBON-FIBER

MICROELECTRODES: TOWARDS AN ONLINE SPECIATION SENSOR

A relationship between FSCV response, free Cu(II) and complexation constant of ligands were modeled to create a relationship to provide useful speciation information in real environmental samples. I contributed both experimentally and intellectually and the results of this project directed me to continue this work on different metals.
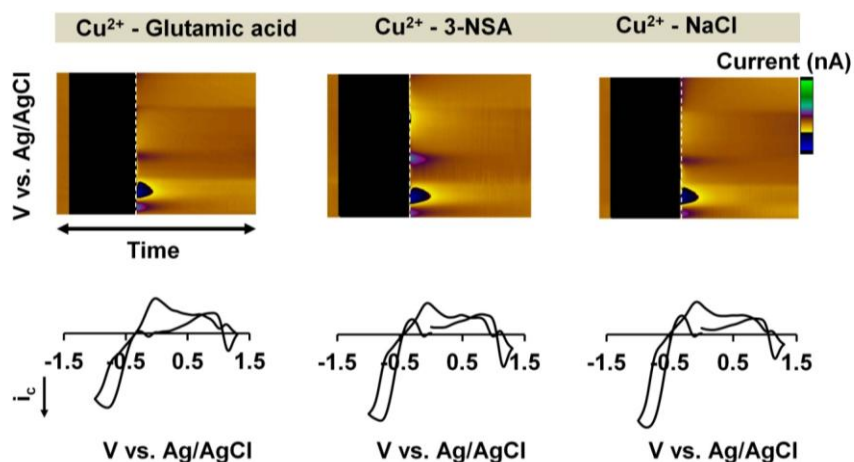
Pathirathna, P.; **Siriwardhane, T**.; Morgan S.L.; McElmurry, S. P.; Hashemi, P.; "Fast voltammetry of metals at carbon-fiber microelectrodes: towards an online speciation sensor"., Analyst 2016, 141, 6432. Reprinted with permission from Copyright(2016), Royal Chemical Society.

4.1 Abstract

Speciation controls the chemical behavior of trace metals. Thus, there is great demand for rapid speciation analysis in a variety of fields. In this study, we describe the application of fast scan cyclic voltammetry (FSCV) and fast scan adsorption controlled voltammetry (FSCAV) for trace metal speciation analysis. We show that Cu(II) can be detected using FSCAV in different matrices. We find that matrices with different Cu(II) binding ability do not affect the equilibrium of Cu(II) adsorption onto CFMs, and thus are an excellent predictor for free Cu(II) ($[Cu(II)]_{free}$) in solution. We modeled a correlation between the FSCV response, $[Cu(II)]_{free}$ and log K_f for 15 different Cu(II) complexes. Using our model, we rapidly predicted, and verified $[Cu(II)]_{free}$ and K_f of a real groundwater sample spiked with Cu(II). We thus highlight the potential of FSCV/FSCAV as a rapid trace metal speciation sensor.

4.2 Introduction

Speciation controls the behavior of metals in real biological and environmental systems. Particularly, it is free, unbound metals in aquatic environments that are readily uptaken by organisms and plants, where at sufficient concentrations they can be pervasively detrimental. Similarly, unbound metals play fundamental roles in biological systems, acting as important signaling molecules.[1] In both environmental and biological systems the concentrations of unbound metals fluctuate dynamically, making it very difficult to define the exact nature and roles of metals in these networks.

Electrochemistry is a promising tool for metal analysis in real, dynamically fluctuating systems because the analysis occurs at an electrode surface which can be fashioned into a variety of, minimally invasive, shapes and sizes. This electrode can easily be submersed or integrated into the system of interest and sample collection can be avoided. While Hg electrodes continue to provide unparalleled sensitivity, they are not easily portable and may pose health hazards. Thus, ion selective electrodes (ISEs) have been intensively used by environmental scientists to investigate metal speciation.[2-4] However, the temporal resolution of ISEs cannot capture dynamic events where metals are rapidly mobilized and transported into environmental waters (e.g. within seconds during storms). Additionally ISE's are not generally suitable for monitoring physiological chemistry in intact systems because of their large dimensions (creating tissue damage).

In recent years, we pioneered fast scan cyclic voltammetry (FSCV) at carbon-fiber microelectrodes (CFMs) for real-time measurements of Cu(II) and Pb(II).[5, 6] A robust adsorption equilibrium on the CFM surface (K_{ads}) allowed us to study Cu(II) complexation with a range of ligands and create a predictive model correlating the FSCV response to overall solution formation constant, K_f.[7] For that prior model to have real-world utility, free Cu(II) concentration ($[Cu(II)]_{free}$) must be known. In this paper, we utilize fast scan constrolled adsorption voltammetry (FSCAV) to characterize $[Cu(II)]_{free}$ and develop a model that relates a single sample FSCV and FSCAV analysis to $[Cu(II)]_{free}$ and K_f. The experiments here first verify that the FSCAV Cu(II) signal is consistent in a

variety of media. Next, we show that different media do not affect Cu(II) adsorption onto CFMs, hence surface coverage is an excellent index of $[Cu(II)]_{free}$. We next fit FSCV and FSCAV data for Cu(II) complexed with 15 different ligands encompassing a wide range of K_fs with a polynomial function to find a correlation between FSCV current, $[Cu(II)]_{free}$, and log K_f. We back-predict the literature K_f values of the 15 ligands and, a signal-to-noise ratio of 19.4, indicates that the model is adequate to make predictions over the range of factor levels investigated. Finally, we use our method to report $[Cu(II)]_{free}$ and K_f in a ground water sample spiked with Cu(II). Our measurement of free $[Cu(II)]_{free}$ is verified with a commercially available ISE. Our findings highlight the important potential of FSCV/FSCAV as a rapid speciation sensor in real samples.

4.3 Experimental Section

4.3.1. Solutions

All chemicals were purchased from Sigma-Aldrich (St. Louis, MO) unless otherwise specified. $Cu(NO_3)_2$ was used as Cu(II) source. Ethylenedaminetetraacetic acid (EDTA), 5-nitrosalicylic acid (5-NSA), 3-nitrosalicylic acid (3-NSA), salicylic acid , oxalic acid, glycine (GLY), dimethylglycine (DMG), nitrilotriacetic acid (NTA), salicylaldehyde, valine (VAL), 2-Ethylidene-1,5-dimethyl-3,3-diphenylpyrrolidine (EDDP), diethylenetriaminepentaacetic acid (DTPA), ethylene glycol-bis(2-aminoethylether)-N,N,N',N'-tetraacetic acid (EGTA), 3,4-dihydroxybenzoic acid (DBA) and glutamic acid were used as model ligands for Cu(II) – ligand

complexation processes. The Cu(II) – ligand mixtures were prepared in 1:1 stoichiometric ratio in NaCl (0.01 M) prior to voltammetric experiments at room temperature and pressure. Sufficient time (>2 h) was given for each solution mixture to come close to steady-state equilibrium prior to experimentation. The pH of each mixture was included in the speciation analysis performed using PHREEQCi.

4.3.2 Microelectrodes

CFMs were constructed as previously described.[8] In brief, a carbon fiber (5 μm radius, T-650, Cytec Industries, NJ) was vacuum aspirated into a glass capillary (0.6 mm external diameter, 0.4 mm internal diameter, A-M Systems, Inc., Sequim, WA). The fiber - filled capillary was pulled with a vertical micropipette puller (Narishige, Tokyo, Japan) to form the carbon-glass seal under the gravity. The pulled electrodes were cut to approximately 150 μm (for FSCV) or 20-55 μm (for FSCAV) under an optical microscope.

4.3.3 Flow Injection Analysis

Flow injection analysis was performed in a custom built system. A CFM was inserted to flangeless short 1/8 nuts (PEEK P-335, IDEX, Middleboro, MA) exposing a small portion of the tip (2 mm) outside of the nut. The nut containing microelectrode was fastened to one end of a modified HPLC union (Elbow PEEK 3432, IDEX, Middleboro, MA). The other end of the elbow union was fastened to the out-flowing stream of the FIA buffer. The reference electrode and the 'waste' flow stream were incorporated via two holes drilled in the union. The flow of the

buffer was maintained with a syringe infusion pump (KD Scientific, Model KDS-410, Holliston, MA). A six-port HPLC loop injector (Rheodyne Model 7010 valve, VICI, Houston, TX) was used to introduce the analyte into the flow stream for 10 seconds as a rectangular pulse.

4.3.4 Fast Scan Cyclic Voltammetry

FSCV experiments were performed with a potentiostat (Dagan Corporation, Minneapolis, MN, USA) and a custom-built breakout box, with national instruments data acquisition cards, for potential and filter application, and current transduction. A custom built software (Knowmad Technologies LLC, Tucson, AZ) was used to collect data, analysis with background subtraction, signal averaging and digital filtration. All voltammetric experiments emloyed a 2-electrode system. A Ag/AgCl electrode constructed by plating Cl- ions on a Ag wire served as the combined counter/reference electrode. Cu(II) cyclic voltammograms (CVs) were collected with an optimized Cu(II) waveform (-1.0 V – +1.3 V at 100 Hz, resting potential of 0 V, at 600 V s^{-1}). Each experiment was repeated using four electrodes with three replicates per electrodes.

4.3.5 Solution Chemistry

The solution chemistry of Cu(II) – ligand mixtures in NaCl was predicted as previously reported[7, 8] using PHREEQCi, a geochemical modeling software (available at the following URL for free) (http://wwwbrr.cr.usgs.gov/projects/GWC_coupled/phreeqc/). The Equilibrium constants required to anticipate the speciation of each of the ligand mixtures

were based on the MINTEQ.v4 database developed by the U.S. Environmental Protection Agency.[9,10] The additional constants for complexation with solutions were modelled in equilibrium with $CO_2(g)$ ($10^{-4.8}$ atm.) and $O_{2(g)}$ ($10^{-0.67}$ atm.).[11]

4.3.6 Fast Scan Controlled-Adsorption Voltammetry

FSCAV experiments were performed as previously described.[12] Briefly, the applied waveform (-1.0 V – +1.3 V at 100 Hz, resting potential of 0 V, at 600 V s^{-1}) on a CFM placed in a Cu(II)-ligand solution was switched to a constant potential of 0 V for 10 seconds, using an electronic relay (ADG-419, Analogue Devices). The total adsorbed copper was quantified by integrating the reduction peak of the first background-subtracted copper cyclic voltammogram (CV) with in house LabVIEW 2012 software. Faraday's law was employed to convert total charge to a surface concentration (Γ_{Cu}), and the measured data was fitted with the linearized Langmuir isotherm (eq. 4.1) where C is the [Cu(II)] in bulk solution, Γmax is the maximum monolayer surface coverage, and K is the equilibrium constant for adsorption.

$$C/\Gamma_{Cu} = (1/\Gamma_{Max})C + 1/(\Gamma_{Max} K) \tag{eq.4.1}$$

4.3.7 Cu(II) Ion Selective Electrode

A Cu(II) calibration curve was constructed with a Copper Combination Ion Selective Electrode (model 4230-A49, Thomas Scientific, Swedesboro, NJ, USA). A series of concentrations of Cu(II) solutions were prepared from a standard Cu(II) solution (1000 ppm, Thomas Scientific, Swedesboro, NJ, USA).

All solutions were stirred well and allowed 20 mins to stabilize before measurement.

4.3.8 Modeling and Statistical Analysis

Prediction modeling of log K_f values as a function of the molar concentration of free Cu(II) in solution and FSCV current was performed using Design Expert, version 10 (Stat-Ease, Inc., Minneapolis, MN). The response surface was estimated using multiple regression for a polynomial model, as described in detail in the discussion section, to test whether log K_f values could be predicted from the Cu(II) concentration and current values.

4.4 Results and Discussion

4.4.1 Voltammetric Determination of Unbound Cu(II)

In both environmental and biological systems, there is a discrepancy between the total concentration of Cu(II) and the concentration of Cu(II) available to engage in chemical processes. Biologically, Cu(II) is rapidly stabilized by proteins, thus only a small percentage of total Cu(II) is thought to be unbound and participating in dynamic processes such as neurotransmission.[13,14] Environmentally, natural organic and inorganic ligands bind Cu(II), while it is generally the free Cu(II) that is readily transported between systems creating harmful effects. Thus, to decipher the roles of Cu(II), it is important to measure its unbound levels as rapidly as possible. Several analytical approaches have been taken to examine this type of speciation including copper-ISEs, potentiometry, cation exchange resins and charge separation techniques.[2,15,16] These methods

generally do not have adequate time resolution to assess the dynamic changes we are interested in deciphering.

In this work, we utilized FSCAV, an extension FSCV,[12] to quantify ambient analyte levels. In FSCAV, a controlled adsorption time period allows ambient Cu(II) to come to equilibrium at the CFM surface, with an equilibrium constant that we refer to as K_{ads}, and thus directly reports the unbound analyte concentration surrounding the CFM. The temporal limitations here are those of file collection and controlled adsorption times such that readings can be taken every 30 seconds. Compared with the tens of minutes required to reach steady state for other speciation analysis methods (vide supra), this temporal resolution represented an improvement of orders of magnitude. To illustrate the applicability of FSCAV to Cu(II) speciation analysis, 1:1 mixtures of Cu(II) – NaCl, Cu(II) – 3-NSA and Cu(II) – Glutamic acid, where Cu(II) was added at a concentration of 0.05 µM, were analyzed. The presence of a characteristic reduction event in the same position on all three color plots (Figure 4.1A) and the cathodic peak around -0.7 V on all three CVs (Figure 4.1B) confirms detection of the same species (Cu(II)) in each mixture.

The differences in the peak height are likely caused by differences in $[Cu(II)]_{free}$ due to the different inherent binding capability of each mixture and excitingly could potentially be used to quantify free Cu(II) in each solution. However, to accurately translate the FSCAV response to $[Cu]_{free}$, it is critical to show that the Cu(II) – CFM equilibrium (K_{ads}) is not affected by the differing equilibria present in different solutions.
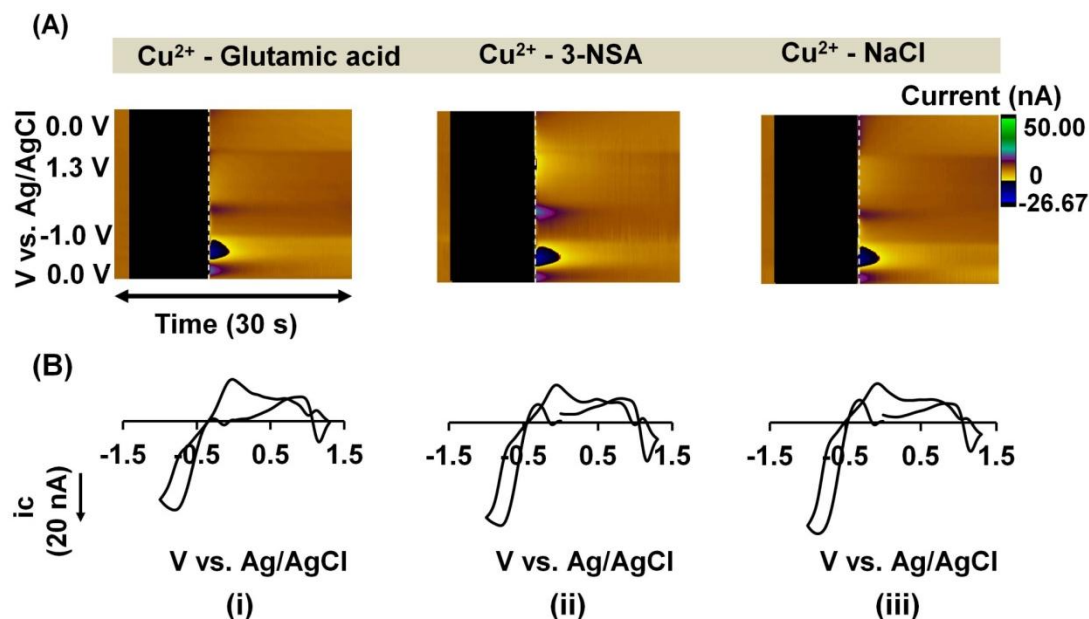
Figure 4.1. Top (A): Representative color plots for (i) Cu(II) – Glutamic acid, (ii) Cu(II) – 3-NSA and (iii) Cu(II) – NaCl complexes with FSCAV. Bottom (B): Buffer subtracted first CV taken at the vertical white dashed lines on color plots.

4.4.2 Cu(II) – CFM K_{ads} is Consistent in Different Media

[Cu(II)]$_{free}$ in solution depends on a variety of factors, including the inherent binding ability of the matrix. In Figure 4.1, differences in FSCAV peak height implied differences in [Cu(II)]$_{free}$, but to pursue the FSCAV response as a basis for quantifying [Cu(II)]$_{free}$ one must assume that different matrices do not alter the K_{ads} of the Cu(II) – CFM equilibrium. This assumption can be held true if we find that for the same [Cu(II)]$_{free}$ in different solutions, the Cu(II) coverage of the CFM surface is the same. We had seen this previously for Cu(II) in tris and NaCl,[8] and in EDTA, citric acid and 5-NSA.[7] Here, we extended the range of media to include 10 solutions with differeing Cu(II) binding abilities. We prepared solutions of different [Cu(II)] in oxalic acid, salicylaldehyde, valine, 3-NSA,

Glycine, DTPA, EGTA, NTA, EDDP and DMG since these matrices all have different affinities for Cu(II). In Figure 4.2 we utilized PHREEQCi to calculate $[Cu(II)]_{free}$ in each solution and plotted this on the x-axis vs. surface coverage, as calculated via Faraday's law and integration of the FSCAV peak.

It is seen that the same $[Cu(II)]_{free}$, regardless of matrix, yields the same CFM surface coverage, demonstrating that the matrices employed in this study do not affect Cu(II) – CFM K_{ads}. We can thus utilize the FSCAV response (surface coverage calculated from peak integration) to report $[Cu(II)]_{free}$ in solutions with differing Cu(II) binding capacities.

Statistics of the fit of the model of surface coverage as a function of free $[Cu(II)]$ confirm a reliable model for prediction. The intercept parameter is estimated to be 11.47 with a 95% confidence interval of 10.22 to 12.71; the estimated slope parameter is 5.58×10^7 with a 95% confidence interval of 5.35×10^7 to 5.80×10^7. Coefficient of determination, R^2 is 0.98, i.e., the factor effect (slope) in the calibration model explains 98 % of the variability in the data about the mean. The coefficient of correlation, R is 0.99.

The ability to report $[Cu(II)]_{free}$ is a powerful analytical development. We previously reported a simple model that could predict the overall solution K_f from FSCV response.[7] Below we illustrate how this relationship is dependent on $[Cu(II)]_{free}$ and thus how FSCV and FSCAV can be utilized to provide multiple levels of speciation information by reporting $[Cu(II)]_{free}$ and overall solution K_f.
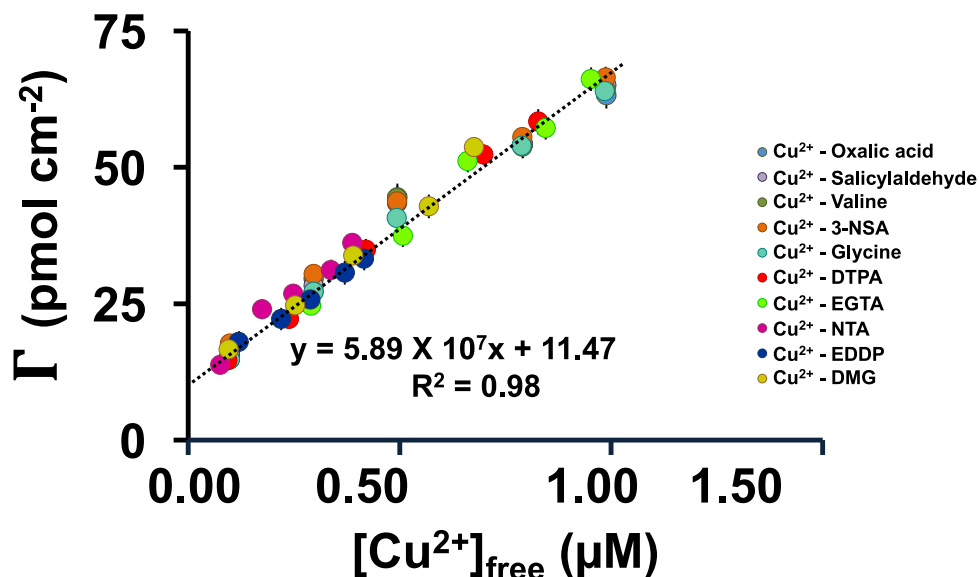
Figure 4.2. Correlation between surface concentration (τ_{Cu}) and [Cu(II)]$_{free}$ in different Cu(II) – ligand solutions. Each color represents individual solution mixtures as depicted in the legend. [Cu(II)]$_{free}$ is calculated via PHREEQCi and surface concentration (y-axis) at each concentration is calculated by integrating cathodic peak on CVs obtained with FSCAV.

4.4.3 FSCV and FSCAV for Multi-Level Speciation Analysis

In a previous study, we showed that the FSCV response could predict the overall K_f of solution by performing experiments where we separately pre-mixed 16 different ligands with a known concentration of Cu(II), performed FIA and obtained a FSCV response.[7] We then constructed a plot between FSCV response and literature reported formation constants and we successfully predicted the K_f of a solution of Cu(II) – Aspartic acid.[7]

A caveat to this previous analysis is that the FSCV response depends on two factors; the [Cu(II)]$_{free}$ and the K_f. Although it is possible to calculate [Cu(II)]$_{free}$ via PHREEQCi in a solution whose composition is known (which we

did in this prior study), for analysis of real samples this approach is not appropriate since the matrix composition is unknown. Therefore, we sought to extend the prior relationships that we found to include $[Cu(II)]_{free}$. In this way, analysis of an unknown sample could yield values for $[Cu(II)]_{free}$ and K_f.
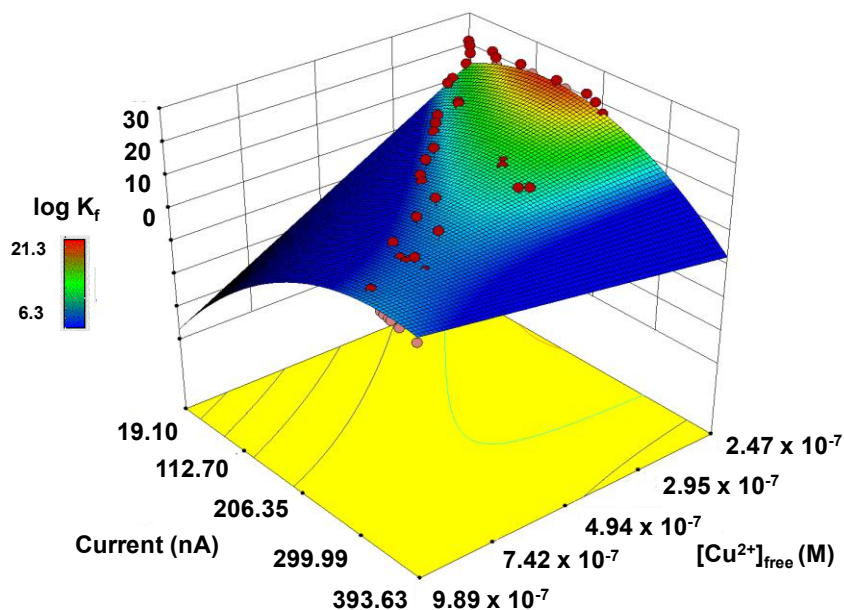
Figure 4.3. Correlation between FSCV response (current), $[Cu(II)]_{free}$ and K_f. Dark red dots represent the design points above the predicted values and pink points represent the design points below the predicted values.

We prepared five different 1:1 concentration series (0.10, 0.30, 0.50, 0.80 and 1.0 µM) of 15 Cu(II) – ligand solutions with known Cu(II) – ligand K_f. We analyzed each mixture with FSCAV and FSCV respectively, with FSCAV providing a value for $[Cu(II)]_{free}$. We used Design Expert, a commercially available statistical software to define the correlation between three parameters; FSCV current, log K_f and $[Cu(II)]_{free}$. We then employed FSCV current and $[Cu(II)]_{free}$ to predict log K_f values (the 'response') for the different ligands (compared to

literature values).[17,18] For each of the ligands, five replicate measurements of the free [Cu(II)] and the measured cathodic current were associated with the respective log K_f values. This analysis is shown in Figure 4.3.

Multiple regression analysis was conducted using a full second-order polynomial model containing an intercept parameter, first order and second order parameters for the two factors, and a Cu(II) – current interaction parameter. This six- parameter empirical model does not represent the underlying mechanism of the system, but is intended to provide a visualization of the factor effects and the capability of the model to predict log K_f values.

Analysis of variance of the partial sum of squares (type III) were used to select parameters having significant effects on the response.[19] All six parameters estimates were found to be statistically different from zero ($p < 0.05$). The significance of the regression showed that the chosen model was significant, with a 0.01 % chance for the calculated F-value of 43.71 to have occurred as a result of noise. The fraction of variance about the mean (R^2) was 0.76, which indicates that appreciable variability was not explained the model. On the other hand, the standard deviation of residuals was only 5.5, a value that is clearly lower than the standard deviation of residuals of 9.11 for our previous model of cathodic current as a function of log K_f values.[7] The model also exhibits a signal-to-noise ratio of 19.4, indicating that the model is adequate to make predictions over the range of factor levels investigated. In the original units of each factor, the equation of the model is:

log10(K_f) = 12.21 − (5.49 x 10^7) x [Cu(II)]$_{free}$ + (0.12) x Current + (1.74 x 105) x [Cu(II)]$_{free}^2$ x Current + (8.82 x 10^{11}) x [Cu(II)]$_{free}^2$ − (4.21 x 10^{-4}) x Current^2

(eq.4.2)

This resulting response surface for prediction of log K_f is shown in Figure 4.3. The log of values, ranging from 6.3 to 21.3, is distributed along a rising diagonal ridge from the front corner to the back corner of the surface as both [Cu(II)]$_{free}$ and current decrease. The plotted data points represent either log K_f values that are higher (red) or lower (pink) than that predicted by the model surface.

4.4.4 Determinaton of [Cu(II)]$_{free}$ and K_f in a Real Environmental Sample

We obtained a groundwater sample collected from Indian Springs Metro Park, MI. We tested this sample with FSCV and FSCAV and found no detectable levels of Cu(II); therefore, we spiked the sample with 0.50 µM Cu(II). FSCV and FSCAV were performed on this spiked sample (4 electrodes (3 replicates on each)) and the average surface concentration was calculated for a total of 12 replicates. [Cu(II)]$_{free}$ was determined with FSCAV to be 0.08 ± 0.01 µM and log K_f was determined with our model as 11.02.

Our predicted overall K_f is importantly, very consistent with prior studies on groundwater (Figure 4.4B).20, 21 The difference in [Cu(II)]$_{added}$ and [Cu(II)]$_{free}$ is due to the removal of [Cu(II)]$_{free}$ via complexation ligands present in groundwater. We verified our [Cu(II)]free result with a commercially available Cu(II) ISE. Figure 4.4A represents the calibration curve constructed for the Cu(II) ISE after an

equilibrium period of 20 minutes. This calibration was performed to verify that there is a linear reponse in groundwater (since the ionic strength is not known and ISE responses are highly very dependent on ionic strength).[22] A slope of 30 mV in the line equation indicates a linear Nernstian response for Cu(II). As observed in the table in Figure 4.4B, the close agreement between our prediction of $[Cu(II)]_{free}$ and the ISE verifies the accuracy of our method.

(A)

$$y = 30.60x + 355.98$$
$$R^2 = 0.99$$

(B)

Ground Water	FSCAV calibration	ISE calibration
Free $[Cu^{2+}]$ / (μM)	0.08 ($\pm$0.01)	0.08 ($\pm$7.00 X 10^{-3})
	Model (predicted)	**Literature**
Log K_f	11.02	11.19[20]
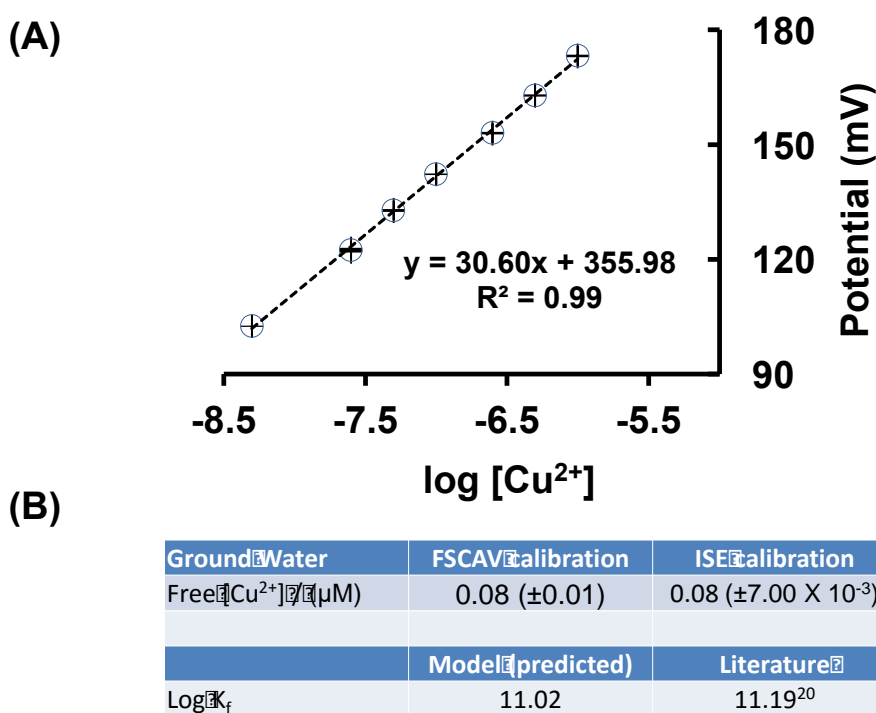
Figure 4.4: (A) Calibration curve for Cu(II) ISE. Line equation represents a perfect Nernstian response with a slope of 30 mV. (B) Summary and a comparison of $[Cu(II)]_{free}$ and log K_f predicted for a groundwater sample using FSCAV and our model represented by eq 4.2.

Our findings show great promise for rapid speciation sensing, and future experiments will study the dependency of various stoichemetric ratios between Cu(II) and ligand and the effect of pH on FSCV and FSCAV responses. Further,

a comprehensive mathematical study is required to incorporate all possible variables into future correlations that could potentially affect our responses to predict speciation information in real systems. Nonetheless, our model excitingly shows that FSCV/FSCAV can be used to rapidly provide multiple levels of speciation information in authentic samples.

4.5 Conclusions

In this paper, we described the application of fast voltammetric tools for Cu(II) speciation analysis. This method can be extended to other metals. We showed that by using FSCAV Cu(II) could be measured in different matrices. We found that matrices with different Cu(II) binding ability did not affect the equilibrium of Cu(II) adsorption onto CFMs, and thus predicted free Cu(II) in solution. We found a relationship between the FSCV response, $[Cu(II)]_{free}$ and log K_f for different Cu(II) complexes. Via this relationship, we rapidly predicted, and verified the free Cu(II) and K_f of a real groundwater sample spiked with Cu(II). We thus present FSCV and FSCAV's promise towards a rapid speciation sensor.

4.6 References

(1) Que, E. L.; Domaille, D. W.; Chang, C. J. *Chemical Reviews* 2008, 108, 1517-1549.

(2) Sauvé, S.; McBride, M.; Hendershot, W. *Archives of Environmental Contamination and Toxicology* 1995, 29, 373-379.

(3) Buffle, J.; Greter, F. L.; Haerdi, W. *Analytical Chemistry* 1977, 49, 216-222.

(4) Lake, D.; Kirk, P.; Lester, J. *Journal of Environmental Quality* 1984, 13, 175-183.

(5) Pathirathna, P.; Yang, Y.; Forzley, K.; McElmurry, S. P.; Hashemi, P. *Analytical Chemistry* 2012, 84, 6298-6302.

(6) Yang, Y.; Pathirathna, P.; Siriwardhane, T.; McElmurry, S. P.; Hashemi, P. *Analytical Chemistry* 2013, 85, 7535-7541.

(7) Pathirathna, P.; Siriwardhane, T.; Morgan, S. L.; McElmurry, S. P.; Hashemi, P. *The Analyst* 2016.

(8) Pathirathna, P.; Samaranayake, S.; Atcherley, C. W.; Parent, K. L.; Heien, M. L.; McElmurry, S. P.; Hashemi, P. *The Analyst* 2014, 139, 4673-4680.

(9) Allison, J. D., Brown, D.S.,Novo-Gradac, K.J. MINTEQA2/PRODEFA2--A Geochemical Assessment Model for Environmental Systems--version 3.0 User's Manual,Environmental Research Laboratory, Office of Research and Development, U.S. Environmental Protection Agency 1990, 106.

(10) Mercê, A.; Mangrich, A.; Szpoganicz, B.; Levy, N.; Felcman, J. *Journal of the Brazilian Chemical Society* 1996, 7, 239-245.

(11) Aslamkhan, A. G.; Aslamkhan, A.; Ahearn, G. A. *Journal of Experimental Zoology* 2002, 292, 507-522.

(12) Atcherley, C. W.; Laude, N. D.; Parent, K. L.; Heien, M. L. *Langmuir* 2013, 29, 14885-14892.

(13) Nalbandyan, R. *Neurochemical research* 1983, 8, 1211-1232.

(14) Porter, H.; Ainsworth, S. *Journal of Neurochemistry* 1961, 7, 20-25.

(15) Stevenson, F.; Chen, Y. Soil Science Society of America Journal 1991, 55, 1586-1591.

(16) Ghaedi, M.; Ahmadi, F.; Soylak, M. *Journal of Hazardous Materials* 2007, 147, 226-231.

(17) Furia, T. E. *CRC Handbook of Food Additives*; CRC press, 1973; Vol. 1.

(18) Analytical and Biological Products Catalog 2012, Dojindo Molecular Technologies, Inc.,Washington, D.C. 252-253.

(19) Deming, S. N.; Morgan, S. L. *Experimental Design: A Chemometric Approach; Elsevier*, 1993; Vol. 11.

(20) Lu, Y.; Allen, H. E. *Water Res* 2002, 36, 5083-5101.

(21) Holm, T. R. *Chemical Speciation & Bioavailability* 1990, 2, 63-76.

(22) De Robertis, A.; Di Giacomo, P.; Foti, C. *Analytica chimica acta* 1995, 300, 45-51.

CHAPTER 5

RAPID ELECTROCHEMICAL ANALYSIS OF Ca(II), Al(III), Zn(II), Mg(II) VIA FAST-SCAN CYCLIC VOLTAMMETRY AT CARBON-FIBER MICROELECTRODES
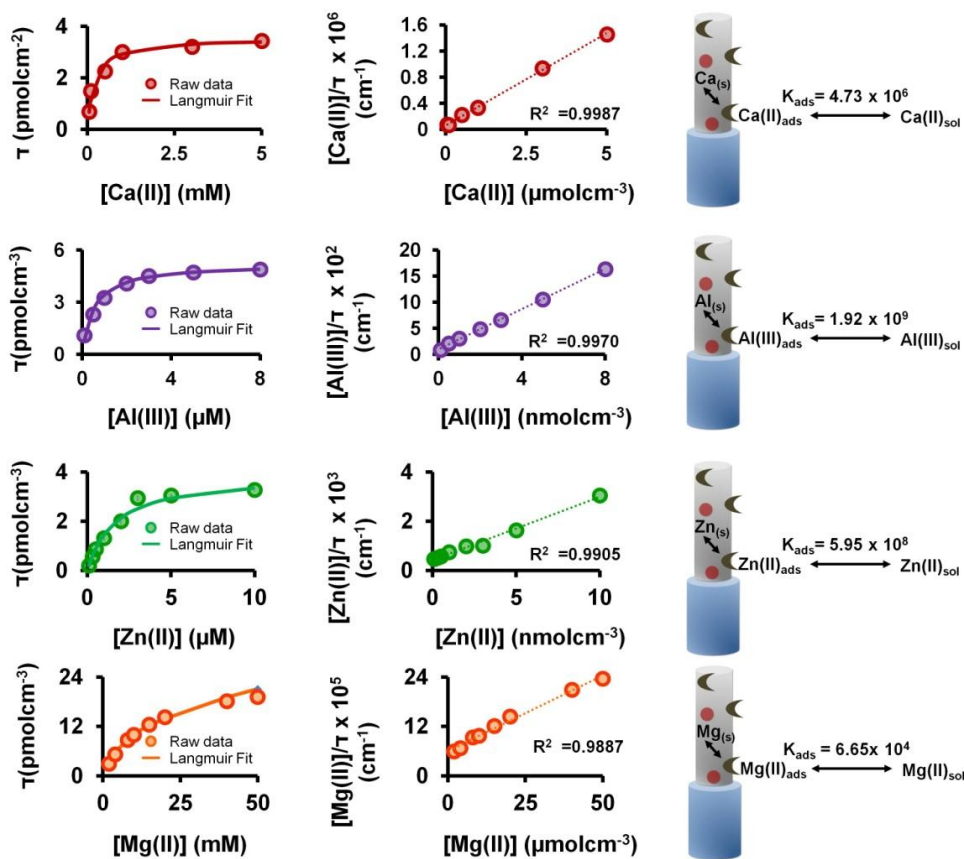
Siriwardhane, T.; Pathirathna, P.; Hashemi, P.: "Rapid Electrochemical Analysis of Ca(II), Al(III), Zn(II), Mg(II) via Fast-Scan Cyclic Voltammetry at Carbon-Fiber Microelectrodes" – In preparation - Analytical Chemistry

5.1 Abstract

Electrochemistry is a powerful approach for simple, low cost metal analysis. However, metals with high negative redox potentials such as Ca(II), Al(III), Zn(II), and Mg(II) are difficult to analyze with traditional electrochemical methods due to the insufficient potential windows associated with common electrode substrates. To introduce a low cost, less laborious approach, we explore fast-scan cyclic Voltammetry (FSCV) at carbon fiber microelectrodes (CFMs) to characterize Ca(II), Al(III), Zn(II), and Mg(II) in real-time. Next, we study the adsorption profiles of these metals via fast-scan controlled-adsorption voltammetry (FSCAV) and establish that all metals follow Langmuir adsorption. Further, we compare the adsorption constants of these metals to literature reported order of sequences for other activated carbon materials to show that they follow the same order of sequence.for adsorption. Finally, we investigate the real-time complexation of these metals with two model ligands, BAPTA (1,2-bis(o-aminophenoxy)ethane-N,N,N′,N′-tetraacetic acid) and EDTA (Ethylenediaminetetraacetic acid) to demonstrate the selectivity of the metals towards respective fscv peaks . Our data demonstrate the powerful capability of our technique to address analytical challenges that are beyond the traditional scope.

5.2 Introduction

Metal analysis is useful in a variety of laboratory and real world situations. [1-3] Electrochemistry is well suited for metal measurements because small cations

can be electrostatically preconcentrated onto traditional electrode materials for high sensitivity measurements. However, the scope of metals that can be analyzed with traditional electrochemistry is limited to those whose redox potentials fall within the potential window of the working electrode. As such, direct electroanalysis of species with highly negative reduction potentials, such as Ca(II), Al(III), Zn(II), and Mg(II) is challenging.[4,5] Previous electrochemical analysis of these species has been performed via indirect complexation strategies,[6-8] which can be lengthy and laborious.

In recent years, we have been employing fast-scan cyclic voltammetry (FSCV) at carbon fiber microelectrodes (CFM) for Cu(II)[9] and Pb(II) analysis.[10] This method is sensitive and fast because the signal is dependent on *adsorption* of ions onto, rather than *mass transport* to, activated carbon electrodes. We previously studied the carbon fiber – metal adsorption thermodynamic equilibrium thats underlies the FSCV reponse. We found that this adsorption equilibrium facilitates redox processes such that cyclic voltammograms for Cu(II) and Pb(II) can be obtained at high scan rates. In this work, we sought to establish whethere this principle applied to metals that are traditionallty difficult to electrochemically analyze. We show, for the first time, robust reduction peaks within the CFM potential window for Ca(II), Al(III), Zn(II), and Mg(II). We demonstrate that the cyclic voltammograms obtained for these species occur as a function of scan rate. We study the adsorption profiles of these metals using fast-scan controlled-adsorption voltammetry (FSCAV) and explain that their adsorption follows a Langmuir adsorption isotherm similar to the monolayer adsorption of Cu(II)) on

CFM as previously observed.[11] The thermodynamic equilibrium constant for adsorption of metals on CFMs is calculated for each metal and we find that these adsorption constants follow the same order as previously reported by other groups on other activated carbon materials. Finally, we perform a real-time complexation study with BAPTA and EDTA, which preferentially bind divalent and multivalent cations respectively[12-14] to address selectivity of the response. This study highlights FSCV as a versatile electrochemical tool whose analytical scope reaches beyond traditional methods.

5.3 Experimental Section

5.3.1 Solutions

Unless otherwise stated, all chemicals were purchased from Sigma-Aldrich (St. Louis, MO, U.S.A). A 0.01 M sodium chloride (NaCl) solution was used as the background electrolyte. Ca(II), Al(III), Zn(II), and Mg(II) solutions were made by dissolving $Ca(NO_3)_2$, $Al(NO_3)_3$, $Zn(NO_3)_2$, $Mg(NO_3)_2$ in 0.01 M NaCl respectively. Both ligands, EDTA and BAPTA, were prepared using the same concentrated NaCl solution. The solution's pH was recorded as being 4.8 ± 0.2.

5.3.2 Microelectrodes

CFMs were prepared as described elsewhere.[9] Briefly, using vacuum suction, a carbon fiber (5 µm radius, T-650, Cytec Industries, NJ, U.S.A) was inserted into a glass capillary (1.0 mm external diameter, 0.5 internal diameter, A-M systems, Inc., Sequim, WA, U.S.A). A vertical micropipette puller (Narishige,

Tokyo, Japan) was used to pull the fiber - filled capillary, creating a carbon-glass seal. Under an optical microscope, the electrode was cut to 150 μm. The electrodes were cycled for 10 min in 60 Hz and 10min in 10 Hz to activate the surface. Each experiment was repeated with four CFMs, with three trials per electrode.

5.3.3 Cyclic Voltammetry

A 2 electrode system was employed for both slow-scan & fast-scan cyclic voltammetry. For slow-scan cyclic voltammetry (scan rates ≤ 100 mVs^{-1}), a microelectrode was placed into a constantly stirring solution of metal nitrate dissolved in 0.01 M NaCl. A triangular waveform was applied using custom build software, Wildcat CV, written in LAB-VIEW 2014 (National Instruments, Austin, TX). Only solutions for slow-scan cyclic voltammetry were nitrogen-purged prior to experimentation. The Ag/AgCl reference electrode was fabricated by electroplating Cl$^-$ onto a Ag wire (A-M systems, WA). FSCV experiments (scan rates ≥ 50 Vs^{-1}) were conducted with a potentiostat (Dagan Corporation, Minneapolis, MN, U.S.A) and custom-built integreation unit that incorporated data aquision cards. Custom software (WCCV 3.06, written in LABVIEW 2014 by Knowmad Technologies, LLC, Tucson, AZ, U.S.A.) was employed to collect and analyze data using background subtraction, signal averaging, and digital filtration.

5.3.4 Fast-Scan Controlled-Adsorption Voltammetry (FSCAV)

FSCAV experiments were performed consistant with our previous reports.[15] An electronic relay (ADG-419, Analog Device) was used to switch

between the waveform at 100 Hz and a constant potential (resting potential). The delay time for the adsorption of metals onto the CFM was 10 seconds. Data analysis of the buffer-subtracted response curve (current vs voltage) was performed with LabVIEW 2014 software by integrating the reduction peak from the background subtracted cyclic voltamogram of metals. The surface concentration (τ_{metal}) was calculated using Faraday's law. Since Ca(II), Al(III), Zn(II), and Mg(II) followed monolayer adsorption, all data was fit to a linearized Langmuir isotherm (equation 1), where C is the concentration of metal in the bulk solution, τ_{max} is the maximum monolayer adsorption at CFM and K is the equilibrium constant for adsorption.

$$(C/\tau_{metal}) = (1/\tau_{max})C + 1/(\tau_{max}K) \qquad \textbf{(Eq 5.1)}$$

5.4 Results and Discussion

5.4.1 Redox Peaks for Ca(II) and Al(III) on CFMs

Voltammetry generates unique analyte-specific CVs based on redox potentials, as such being an excellent characterization method. However, is it is generally not possible to voltammetrically analyze species whose redox potentials fall outside the potential window of the electrode substrate. A number of important metals, including Ca(II) and Al(III), are considered challenging to electroanalyze with traditional electrode materials due to this constraint.

We previously determined that the adsorption of Cu (II) onto CFMs facilitates the FSCV signal.[11] Here, we asked whether adsorption of metals, that are commonly difficult to analyze, would afford the same phenomenon. Figure

5.1 represents the cyclic voltamograms of 1.0 M Ca(II) (left orange panel) and 0.1 M Al(III) (right blue panel) as a function of scan rate using slow scan (10-100 mVs^{-1}) and background-subtracted fast scan cyclic voltammetry (1 Vs^{-1} and above) at CFMs.

Figure 5.1i shows a very small reduction peak appears at -0.1V at 10 mVs^{-1} for Ca(II). For adsorbed species, increasing scan rate yields higher current and this is the case here as this peak becomes more defined and shifts in the negative direction at faster scan rates. The difference in CV shape on going from
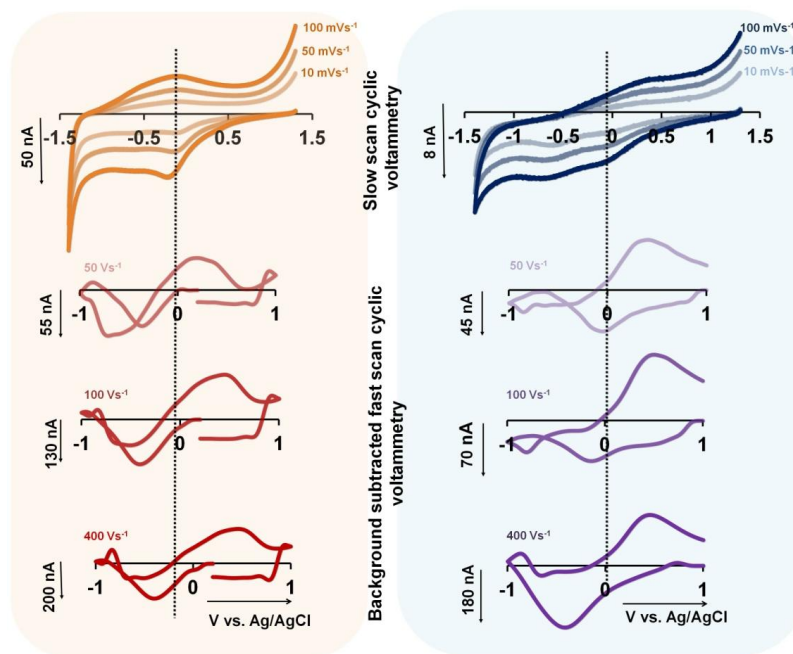
Figure 5.1. Cyclic voltammograms collected for Ca(II)(left orange and red) and Al(III) (right-blue and purple) in increasing scan rates.

slow to fast scan cyclic voltammetry is because of background substraction and the fundamentally different way that FSCV is performed. Nonetheless, this experiment allows us to confirm that adsorption processes unique to CFMs

facilitate redox peaks within carbon's potential window for Ca(II). The same phenomenon holds for Al (III) in Figure 5.1ii. Next we south to establish whether Zn(II) and Mg(II) also display redox peaks on CFMs.

5.4.2 Characterization of Ca(II), Al(III), Zn(II) and Mg(II).

In this experiment, FSCV was performed on Ca(II), Al(II), Zn(II) and Mg(II) in a flow injection analysis (FIA) system. The waveform parameters (potential limits, resting potential and scan rate) were optimized for each metal as in our prior work to obtain a CV with a well-defined reduction peak. Figure 5.2A shows representative color plots obtained for FIA of each metal with their respectively optimized waveforms. A reduction event is apparent for each metal on these color plots.
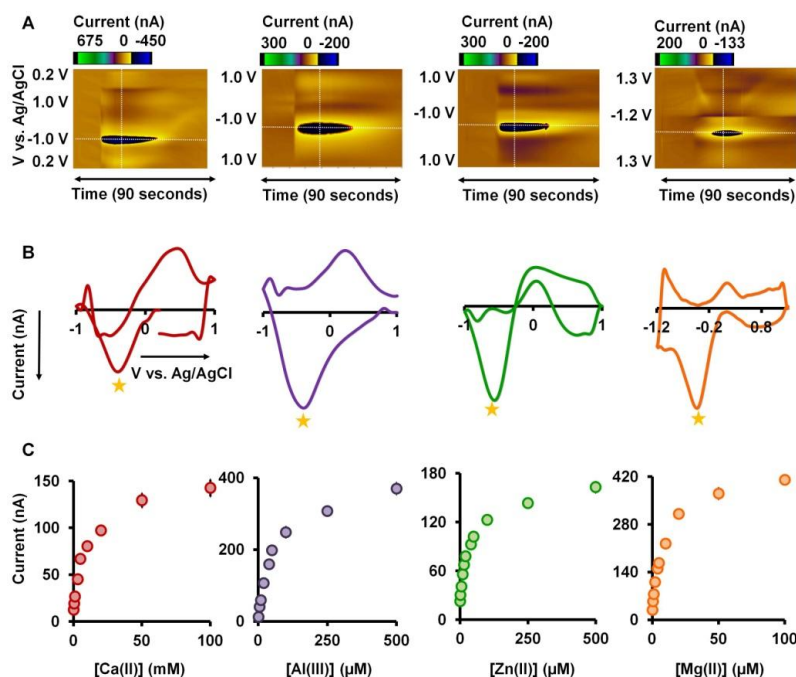
Figure 5.2. FSCV characterization for Ca(II) (red), Al(III) (purple), Zn(II) (green), and Mg(II) (orange). A. Represent color plots for each metal B. Representative CVs C. Calibration curves constructed for each metal.

Figure 5.2B shows CVs reconstructed from the color plots. It is difficult to compare the peak positions and currents between the four because of the different waveforms utilized. However the reduction peaks that appeared at -0.3, -0.4, -0.6 and -0.5 V on Ca(II), Al(III), Zn(II) and Mg(II), respectively, can employed to construct calibration curves (Figure 5.2C) for each metal. The linear range and limit of quantitation (LOQ) for each metal were calculated and are tabulated in Table 5.1. In all cases, the linear range and LOQ are sufficient to analyze a range of physiological and environmental systems.[16-18]

The powerful capability of FSCV to report dynamic levels of these metals directly allows us to use this novel method as a simple, fast laboratory tool. Hence we expand our study to investigate the adsorption profiles of each metal, as discussed in the next section.

Table 5.1. Calibration parameters for the each meal

Metal	Linear range	LOQ
Ca(II)	0.10 - 5.00 mM	0.1 mM
Al(III)	1.00 - 50.00µM	1.00 µM
Zn(II)	0.50 - 20.00 µM	0.50 µM
Mg(II)	0.010 -2.00 mM	0.010 mM

5.4.3 Adsorption Constants onto CFMs are consistent with Adsorption onto Other Activated Carbon Materials.

It is difficult to compare the thermodynamic properties of the different signals because different waveforms were necessary for a well defined reduction peak. However, it is possible to compare adsorption profiles by constructing isotherms and calculating equilibrium constants for metal-CFM adsorption(K_{ads}). We previously reported the adsorption isotherm profile for Cu(II)-CFM which agreed well with a Langmuir adsorption isotherm, suggesting a monolayer of Cu(II) on CFMs.[11] Here we did the same for Ca(II), Al(II), Zn(II) and Mg(II) using FSCAV.

We performed FSCAV experiments for each metal in a simple matrix, NaCl. Although we have reported that the surrounding matrix does not disturb the adsorption of Cu(II) on CFM,[19] we preferred to use a simple matrix here without competing equilibria to simplify this experiment. In Figure 5.3i, a series of different concentrations of each metal (A-D) was prepared in 0.01 M NaCl and the surface concentration of each metal was calculated as explained above.[11] The experimental data fit well to a linearized Langmuir model as shown in Figure 5.3ii, confirming monolayer adsorption. K_{ads} for each metal was calculated using Equation 5.1. Figure 5.3iii represents a schematic diagram that illustrates the adsorption equilibrium and K_{ads} of each metal on CFM. Adsorption favorability of these four metals to CFM was evaluated and compared to the literature reported adsorption to other activated carbon materials. Since our carbon fibers are activated electrochemically by oxidizing at 1.3 V prior to each experiment, we
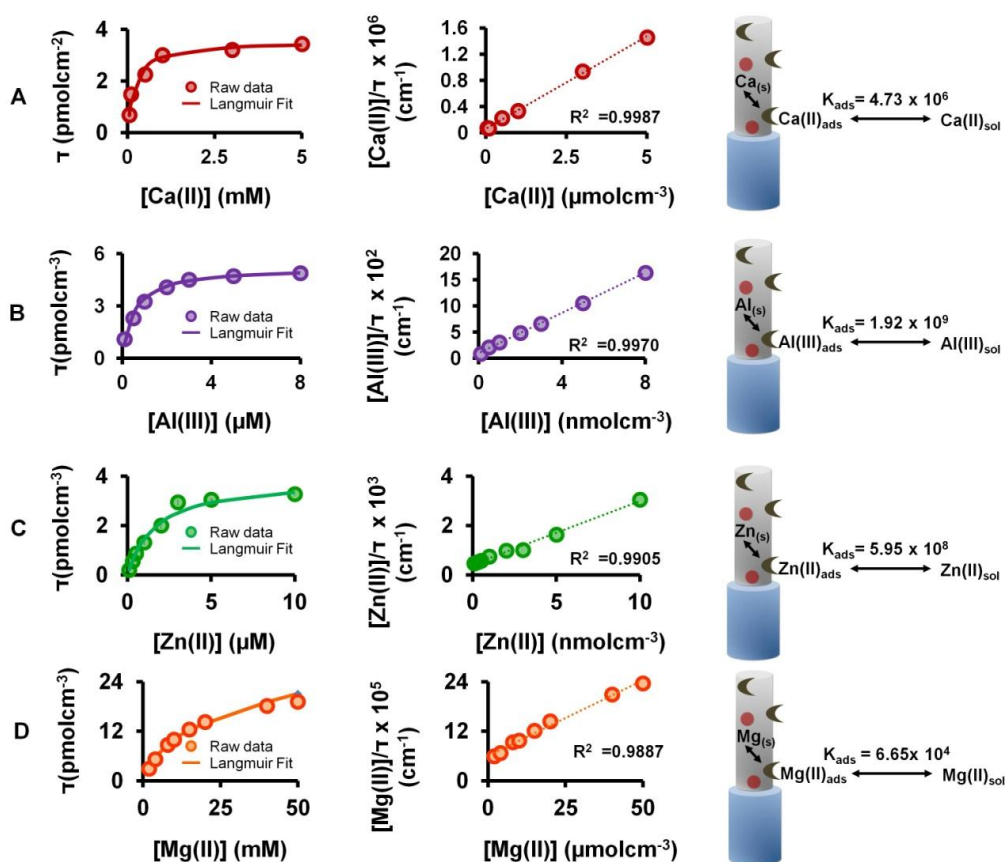
Figure 5.3. Adsorption profiles for (A) Ca(II), (B) Al(III), (C) Zn(II), and (D) Mg(II). i) Langmuir isotherm fit with raw data, ii) linearized Langmuir isotherm and iii) schematic representation of solution equilibria.

hypothesize the order of adsorption should be similar for these four metals as on activated carbon materials that are used to 'remove' metals from aqueous systems. Alkali earth metals adsorb weakly onto activated carbon[20] and our data support this since Mg (II) has the lowest adsorption on CFM followed by Ca(II). We previously studied Cu(II) adsorption and reported the K_{ads} value as 4.12 x 10^9,[11] and here find that Zn(II) has a lower adsorption with a K_{ads} of 5.95 x 10^8. Literature validates this result, showing that Cu(II) adsorption more favorable than Zn(II) onto carbon.[21,22] Comparison of Al (III) adsorption to other metals has

not been reported in the literature. Here we report that Al(III) has a similar adsorption to Cu(II) on carbon fibers. In sum, we report adsorption favorabilities thus: Mg(II) < Ca(II) < Zn((II) < Al(III) ≤ Cu(II).

Our results suggest that most metals follow monolayer adsorption on CFMs and have different adsorption efficiencies based on their size and electrostatic interactions with carbon fibers. It is clear that this adsorption is so favorable such that metals are rapidly brought to the surface allowing for their direct electrochemical analysis with FSCV. In the next section, we study the real-time complexation of these metals with FSCV.

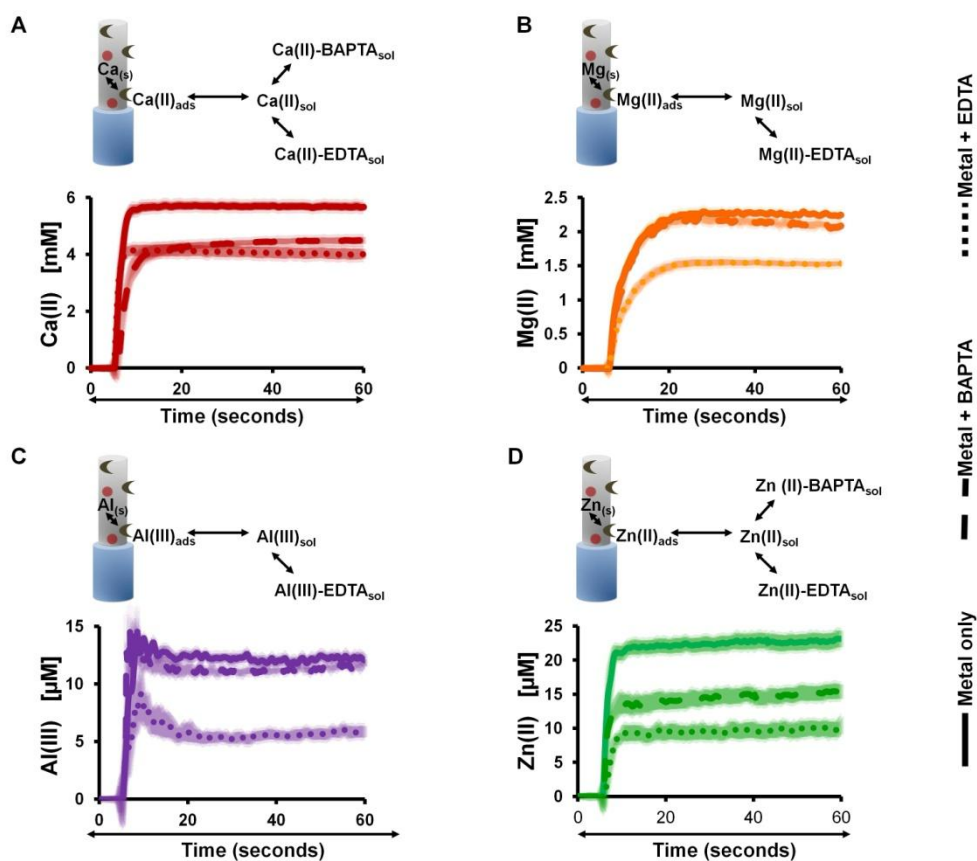### 5.4.4 Real-Time Complexation Studies

To further verify that these FSCV signals are generated directly as a consequence of the metal, rather than erroneously, we performed the following experiment as a proof-of-principle study. Here, we used EDTA and BAPTA as ligands with varying affinities for the four metals. BAPTA has been shown to selectively bind to Ca(II) in a mixture of Ca(II) and Mg(II) serving as a chelator for selective studies of Ca(II) in complex biological matricies. EDTA was chosen as an universal chelator as it binds unselectively to many metals. The experimental paradigm utilized here composed of three steps. Using Ca(II) as an example, an electrode was dipped into a solution of NaCl and allowed to equilibriate. After 5s, Ca(II) was injected into this solution to reach a final concentration of 5 mM. The solid red line on Figure 5.4A illustrates the Ca(II) concentration change over time. Next, two similar experiments were performed but Ca(II) was spiked into a solution of 2.5 mM BAPTA and EDTA respectively. The dashed red line

84

represents the concentration change of Ca(II) when injected into BAPTA and the dotted red line represents the injection into EDTA. The same three steps were carried out for Al(III), Zn(II), and Mg(II) with differing concentrations depending on their linear range and environmental availability. A 2 mM solution was used as the Mg(II) solution shown in Figure 5.4B and 1 mM was used for BAPTA and EDTA. For Al(III), in Figure 5.4C, the final concentration was 10 µM, with 5 µM BAPTA and 5µM EDTA was used in consecutive steps. Figure 5.4D shows the concentration change for Zn(II) during 3 steps. 20 µM Zn(II) and 10 µM BAPTA and 10 µM EDTA were used.

When Ca(II) was spiked into NaCl, the current changed signifying an increase in unbound Ca(II) concentration. Ca(II) was then added to a stirring solution of BAPTA. Since BAPTA binds Ca(II), the unbound [Ca(II)] was lower in this medium than in NaCl. The same process occured with EDTA with Ca(II) settling at a lower level still. This difference is attributed to the higher formaton constant (log K_f) value of Ca(II)-EDTA (10.96) binding vs. Ca(II)-BAPTA binding (6.97).[23]

As in Ca(II), Mg(II) injection to NaCl showed an increase in the current response with respect to Mg(II) concentration. However, Mg(II) did not show any decrease in the current signal compared to in NaCl, when it was spiked to BAPTA solution, rather it showed a lower current response in EDTA solution. This difference is attributed to the low affinity of Mg(II) to BAPTA (K_f 1.77) than to EDTA (K_f 8.69).

Al(II) injection to NaCl followed the same route where an increase in the current was reported due to unbound Al(II) in the solution. As expected, Al(III) injection to BAPTA did not show any decrease in the signal as trivalent cations does not bind with BAPTA. Al(III) injection to EDTA showed a decreased signal differentiating the affinity of Al(II) towards BAPTA and EDTA (K_f 16.13).

Figure 5.4. Schematic representation of different equilibria in each solution (top) and real-time complexation data with EDTA and BAPTA (bottom) for A. Ca(II), B. Mg(II), C. Al(III), and D. Zn(II). The shaded area around each line represents the standard error of mean (SEM) for repetition of 12 data points

Finally Zn(II) was injected to NaCl giving a current change respective to its concentration. The ability of BAPTA to bind divalent cations (except Mg(II))was

verified by the injection of Zn (II) to BAPTA solution which gave a decreased signal than in NaCl. The Zn(II) injection to EDTA followed the same with a larger decrease than BAPTA. The results validated the ability of our technique to differentiate between formation constants of Zn(II) towards BAPTA (K_f 9.38) and EDTA (K_f 16.50).

Collectively, our data serve as evidence that our technique is not only capable of qualitative and quantitative measurements of metals that are traditionally hard to directly measure, but also real-time complexation in a simple medium. In the future, this novel tool can be further modified to characterize metals with high selectivity for real-time in situ measurements in complex natural systems.

5.5 Conclusion

Metals with high negative redox potentials are difficult to study with traditional electrochemical techniques and electrode materials and different complexation strategies combined with spectroscopy and electrochemistry have previously been used. In this study, we employed FSCV to directly characterize Ca(II), Mg(II), Al(III), and Zn(II) in real-time. Further, we utilized FSCAV to analyze their adsorption profiles and reported that the adsorption followed a Langumire adsorption isotherm. The order of the sequence of the equilibrium constants for adsorption between these metals and CFM followed the same order as on other activated carbon materials. Finally, the real-time complexation studies confirmed the validity of our technique by selectively binding with BAPTA

and EDTA. Our findings suggest the strength of our technique as a low cost, real-time sensor for the detection of electrochemically challenging analytes.

5.6 Reference

(1) Tchounwou, P. B.; Yedjou, C. G.; Patlolla, A. K.; Sutton, D. J. *EXS* 2012, 101, 133-164.

(2) Dorne, J. L.; Kass, G. E.; Bordajandi, L. R.; Amzal, B.; Bertelsen, U.; Castoldi, A. F.; Heppner, C.; Eskola, M.; Fabiansson, S.; Ferrari, P.; Scaravelli, E.; Dogliotti, E.; Fuerst, P.; Boobis, A. R.; Verger, P. *Metal ions in life sciences* 2011, 8, 27-60.

(3) Jarup, L. *Br Med Bull* 2003, 68, 167-182.

(4) Economou, A. TrAC Trends in *Analytical Chemistry* 2005, 24, 334-340.

(5) Zhang, F.; Bi, S.; Zhang, J.; Bian, N.; Liu, F.; Yang, Y. *Analyst* 2000, 125, 1299-1302.

(6) Wang, J.; Farias, P. A. M.; Mahmoud, J. S. *Analytica Chimica Acta* 1985, 172, 57-64.

(7) Arancibia, V.; Muñoz, C. *Talanta* 2007, 73, 546-552.

(8) Zhu, J.; Qin, Y.; Zhang, Y. *Analytical chemistry* 2010, 82, 436-440.

(9) Pathirathna, P.; Yang, Y.; Forzley, K.; McElmurry, S. P.; Hashemi, P. *Analytical chemistry* 2012, 84, 6298-6302.

(10) Yang, Y.; Pathirathna, P.; Siriwardhane, T.; McElmurry, S. P.; Hashemi, P. *Analytical chemistry* 2013, 85, 7535-7541.

(11) Pathirathna, P.; Samaranayake, S.; Atcherley, C. W.; Parent, K. L.; Heien, M. L.; McElmurry, S. P.; Hashemi, P. *Analyst* 2014, 139, 4673-4680.

(12) Rousset, M.; Cens, T.; Vanmau, N.; Charnet, P. *FEBS letters* 2004, 576, 41-45.

(13) Mantoura, R. F. C.; Dickson, A.; Riley, J. P. *Estuarine and Coastal Marine Science* 1978, 6, 387-408.

(14) Sillanpää, M.; Oikari, A. *Chemosphere* 1996, 32, 1485-1497.

(15) Atcherley, C. W.; Laude, N. D.; Parent, K. L.; Heien, M. L. *Langmuir* 2013, 29, 14885-14892.

(16) Nagajyoti, P. C.; Lee, K. D.; Sreekanth, T. V. M. *Environmental Chemistry Letters* 2010, 8, 199-216.

(17) Crapper, D. R.; Krishnan, S. S.; Dalton, A. J. *Science* 1973, 180, 511-513.

(18) Parisi, A. F.; Vallee, B. L. *The American journal of clinical nutrition* 1969, 22, 1222-1239.

(19) Pathirathna, P.; Siriwardhane, T.; McElmurry, S. P.; Morgan, S. L.; Hashemi, P. *Analyst* 2016, 141, 6432-6437.

(20) Goldin, M. M.; Volkov, A. G.; Namychkin, D. N.; Filatova, E. A.; Revina, A. A. *Journal of The Electrochemical Society* 2005, 152, E172-E175.

(21) Bouhamed, F.; Elouear, Z.; Bouzid, J.; Ouddane, B. *Environ Sci Pollut Res* 2016, 23, 15801-15806.

(22) Stafiej, A.; Pyrzynska, K. *Separation and Purification Technology* 2007, 58, 49-52.

(23) Analytical and Biological Products Catalog, Dojindo Molecular Technologies, Inc., Washington, D.C., 2012, 252-253.

CHAPTER 6

CONCLUSION AND FUTURE PROSPECTS

Development of novel electrochemical methods with adequate temporal resolution is essential for understanding rapid metal speciation. Traditional techniques suffer from low temporal resolution due to complex sample pretreatment and pre-concentration steps. Additionally, failure to differentiate between free metal concentration from complexed state makes them impractical for speciation studies. Thus, there is a high demand for rapid speciation analysis technique that can provide meaningful data in real-time. We have pioneered the use of FSCV at CFMs to address these issues by optimizing the technique to detect Cu(II). In this dissertation work, we first developed the technique to analyze Pb (II) in different test solutions including storm water run-off. Next, a complexation study between Cu(II) and a model set of ligands was performed to prove FSCV's ability to provide complexation information in real-time which reflects speciation information. This work was extended with a range of ligands to build a mathematical relationship between free Cu(II), FSCV response, and the complexation constant that can be used to provide information in a given solution. Finally, a range of other metals that are difficult to detect using traditional electrochemical techniques, due to their high standard reduction potentials, were rapidly characterized using FSCV. Collectively, our data

represent an important first step towards developing an eco-friendly, handheld, and portable on-site metal speciation sensor.

Future studies will require a series of fundamental characterizations to develop an on-site Cu(II) speciation sensor. The fundamental principles that govern the FSCV and FSCAV response should be addressed. Our study characterized model ligands with a ratio of 1:1 with Cu(II), since most metals bind with Cu(II) in 1:1 ratio. In order to use the sensor in complex natural solutions, a variety of ligands with different stoichiometric ratios should be evaluated. Additionally, the pH dependency should be addressed, as dynamic events can rapidly alter the pH. The ionic strength, steady state equilibria (for FSCAV response) should be evaluated by incorporating all possible dynamic ranges that can be found in natural systems. The selectivity of the electrode towards Cu(II) should be addressed since our technique is not capable of providing the required selectivity for Cu(II). The first steps towards covalently modifying the surface of the electrode using a Cu (II) specific ionophore was introduced by our group in 2016. This modification should be improved to withstand harsh conditions found in dynamic natural systems while also maintaining adequate temporal resolution. Finally, all fundamental characteristics must be modeled and incorporated into a single relationship that can be used for the portable device to provide on-site speciation information in real-time. A collaboration is required to design (physical) the miniaturized handheld portable Cu(II) speciation sensor that is cost effective and easy to use.

Finally, more metals will be evaluated and will be used to design different metal speciation sensors that could accurately describe the speciation of a given solution in real-time. Together, our studies will provide a solid tool for rapid speciation information analysis that could benefit fundamental health, biological and environmental systems.

APPENDIX A

Permission obtained from American Chemical Society to reprint the article in Chapter 2

Permission obtained from The Royal Society of Chemistry to reprint the article in Chapter 3

Fast voltammetry of metals at carbon-fiber microelectrodes: rapid determination of solution formation constants

Pathirathna, P.; Siriwardhane, T.; Morgan S.L.; McElmurry, S. P.; Hashemi, P.: Analyst 2016, 141, 6432

DOI: 10.1039/C6AN01401A

If you are not the author of this article and you wish to reproduce material from it in a third party non-RSC publication you must formally request permission using RightsLink. Go to ourInstructions for using RightsLink page for details.

Authors contributing to RSC publications (journal articles, books or book chapters) do not need to formally request permission to reproduce material contained in this article provided that the correct acknowledgement is given with the reproduced material.

Reproduced material should be attributed as follows:

- For reproduction of material from NJC:
Reproduced from Ref. XX with permission from the Centre National de la Recherche Scientifique (CNRS) and The Royal Society of Chemistry.
- For reproduction of material from PCCP:
Reproduced from Ref. XX with permission from the PCCP Owner Societies.
- For reproduction of material from PPS:
Reproduced from Ref. XX with permission from the European Society for Photobiology, the European Photochemistry Association, and The Royal Society of Chemistry.
- For reproduction of material from all other RSC journals and books:
Reproduced from Ref. XX with permission from The Royal Society of Chemistry.

If the material has been adapted instead of reproduced from the original RSC publication "Reproduced from" can be substituted with "Adapted from".

In all cases the Ref. XX is the XXth reference in the list of references.

If you are the author of this article you do not need to formally request permission to reproduce figures, diagrams etc. contained in this article in third party publications or in a thesis or dissertation provided that the correct acknowledgement is given with the reproduced material.

Reproduced material should be attributed as follows:

- For reproduction of material from NJC:
[Original citation] - Reproduced by permission of The Royal Society of Chemistry (RSC) on behalf of the Centre National de la Recherche Scientifique (CNRS) and the RSC
- For reproduction of material from PCCP:
[Original citation] - Reproduced by permission of the PCCP Owner Societies
- For reproduction of material from PPS:
[Original citation] - Reproduced by permission of The Royal Society of Chemistry (RSC) on behalf of the European Society for Photobiology, the European Photochemistry Association, and RSC
- For reproduction of material from all other RSC journals:
[Original citation] - Reproduced by permission of The Royal Society of Chemistry

If you are the author of this article you still need to obtain permission to reproduce the whole article in a third party publication with the exception of reproduction of the whole article in a thesis or dissertation.

Information about reproducing material from RSC articles with different licences is available on our Permission Requests page.

APPENDIX C

Permission obtained from The Royal Society of Chemistry to reprint the article in Chapter 4

Fast voltammetry of metals at carbon-fiber microelectrodes: towards an online speciation sensor

If you are not the author of this article and you wish to reproduce material from it in a third party non-RSC publication you must formally request permission using RightsLink. Go to our Instructions for using RightsLink page for details.

Authors contributing to RSC publications (journal articles, books or book chapters) do not need to formally request permission to reproduce material contained in this article provided that the correct acknowledgement is given with the reproduced material.

Reproduced material should be attributed as follows:

- For reproduction of material from NJC:
Reproduced from Ref. XX with permission from the Centre National de la Recherche Scientifique (CNRS) and The Royal Society of Chemistry.
- For reproduction of material from PCCP:
Reproduced from Ref. XX with permission from the PCCP Owner Societies.
- For reproduction of material from PPS:
Reproduced from Ref. XX with permission from the European Society for Photobiology, the European Photochemistry Association, and The Royal Society of Chemistry.
- For reproduction of material from all other RSC journals and books:
Reproduced from Ref. XX with permission from The Royal Society of Chemistry.

If the material has been adapted instead of reproduced from the original RSC publication "Reproduced from" can be substituted with "Adapted from".

In all cases the Ref. XX is the XXth reference in the list of references.

If you are the author of this article you do not need to formally request permission to reproduce figures, diagrams etc. contained in this article in third party publications or in a thesis or dissertation provided that the correct acknowledgement is given with the reproduced material.

Reproduced material should be attributed as follows:

- For reproduction of material from NJC:
[Original citation] - Reproduced by permission of The Royal Society of Chemistry (RSC) on behalf of the Centre National de la Recherche Scientifique (CNRS) and the RSC
- For reproduction of material from PCCP:
[Original citation] - Reproduced by permission of the PCCP Owner Societies
- For reproduction of material from PPS:
[Original citation] - Reproduced by permission of The Royal Society of Chemistry (RSC) on behalf of the European Society for Photobiology, the European Photochemistry Association, and RSC
- For reproduction of material from all other RSC journals:
[Original citation] - Reproduced by permission of The Royal Society of Chemistry

If you are the author of this article you still need to obtain permission to reproduce the whole article in a third party publication with the exception of reproduction of the whole article in a thesis or dissertation.

Information about reproducing material from RSC articles with different licences is available on our Permission Requests page.